

1 **Origin Matters: Using a Local Reference** 2 **Genome Improves Measures in Population** 3 **Genomics**

4 *Doko-Miles J. Thorburn^{1,2+}, Kostas Sagonas^{1,3}, Mahesh Binzer-Panchal⁴, Frederic J.J. Chain⁵,*
5 *Philine G.D. Feulner^{6,7}, Erich Bornberg-Bauer⁸, Thorsten BH Reusch⁹, Irene E. Samonte-*
6 *Padilla¹⁰, Manfred Milinski¹⁰, Tobias L. Lenz^{11,12}, Christophe Eizaguirre¹*

7 ¹School of Biological and Chemical Sciences, Queen Mary University of London, London,
8 United Kingdom.

9 ²Department of Life Sciences, Imperial College London, London, United Kingdom.

10 ³Department of Zoology, School of Biology, Aristotle University of Thessaloniki,
11 Panepistimioupoli, 54124 Thessaloniki, Greece.

12 ⁴Department of Medical Biochemistry and Microbiology, National Bioinformatics Infrastructure
13 Sweden (NBIS), Science for Life Laboratory, Uppsala University, Sweden.

14 ⁵Department of Biological Sciences, University of Massachusetts Lowell, USA.

15 ⁶Department of Fish Ecology and Evolution, Centre of Ecology, Evolution and
16 Biogeochemistry, EAWAG Swiss Federal Institute of Aquatic Science and Technology,
17 Kastanienbaum, Switzerland.

18 ⁷Division of Aquatic Ecology and Evolution, Institute of Ecology and Evolution, University of
19 Bern, Bern, Switzerland.

20 ⁸Evolutionary Bioinformatics, Institute for Evolution and Biodiversity, Westfälische Wilhelms
21 University, Münster, Germany.

22 ⁹Marine Evolutionary Ecology, GEOMAR Helmholtz Centre for Ocean Research, Kiel,
23 Germany.

24 ¹⁰Department of Evolutionary Ecology, Max Planck Institute for Evolutionary Biology, Plön,
25 Germany.

26 ¹¹Research Group for Evolutionary Immunogenomics, Max Planck Institute for Evolutionary
27 Biology, Plön, Germany.

28 ¹²Research Unit for Evolutionary Immunogenomics, Department of Biology, University of
29 Hamburg, Hamburg, Germany.

30 ⁺Corresponding author: d.m.j.thorburn@qmul.ac.uk

31 **Abstract**

32

33 Genome-level sequencing enables us to ask fundamental questions about the genetic basis
34 of adaptation, population structure, and epigenetic mechanisms, but usually requires a
35 suitable reference genome for mapping population-level re-sequencing data. In some model
36 systems, multiple reference genomes are available, giving researchers the challenging task
37 of determining which reference genome best suits their data. Here we compare the use of two
38 different reference genomes for the three-spined stickleback (*Gasterosteus aculeatus*), one
39 novel genome derived from a European gynogenetic individual and the published reference
40 genome of a North American individual. Specifically, we investigate the impact of using a local
41 reference versus one generated from a distinct lineage on several common population
42 genomics analyses. Through mapping genome resequencing data of 60 sticklebacks from
43 across Europe and North America, we demonstrate that genetic distance among samples and
44 the reference impacts downstream analyses. Using a local reference genome increased
45 mapping efficiency and genotyping accuracy, effectively retaining more and better data.
46 Despite comparable distributions of the metrics generated across the genome using SNP data
47 (i.e., π , Tajima's D , and F_{ST}), window-based statistics using different references resulted in
48 different outlier genes and enriched gene functions. A marker-based analysis of DNA
49 methylation distributions had a comparably high overlap in outlier genes and functions, yet
50 with distinct differences depending on the reference genome. Overall, our results highlight
51 how using a local reference genome decreases reference bias to increase confidence in
52 downstream analyses of the data. Such results have significant implications in all reference-
53 genome-based population genomic analyses.

54

55 **Keywords:** Reference genomes, population genomics, gynogenetic, genome assembly, read
56 mapping, *Gasterosteus aculeatus*, stickleback, reference mapping bias

57 **Introduction**

58 Genome-level sequencing has revolutionized many biological fields including evolution,
59 ecology, microbiology, and population genomics (M. R. Jones & Good, 2016; Kao et al., 2014;
60 Stapley et al., 2010). Historically, scientists have relied on one or a small number of high-
61 quality reference genomes to address their specific questions. Progressively, the availability
62 of high-quality reference genomes from large-scale projects (e.g., Earth BioGenome and
63 Vertebrate Genome Projects; Lewin et al., 2018; Scientists, 2009), the decreasing costs of
64 sequencing, and the availability of curated variant databases (e.g., dbSNP and dbVar;
65 Lappalainen et al., 2013; Sherry et al., 2001) have improved the breadth and depth of genomic
66 research. However, limitations due to the availability and quality of these resources and the
67 challenge of integrating and interpreting multiple sources of genetic variation still exist
68 (Formenti et al., 2022). These problems are only exacerbated in non-model systems where a
69 high-quality reference genome may not exist. Recently, a graph-based genome alignment
70 methodology has been developed to index and incorporate variant databases, providing a
71 practical and highly efficient method that better captures variation in a genome (Kim et al.,
72 2019). However, databases of high-quality variants are not currently available for most study
73 systems. Moreover, in highly variable regions graph-based approaches can incur significant
74 computational overhead and have an increased chance of false-positive alignments (Grytten
75 et al., 2020; Pritt et al., 2018). Hence, until graph-based methods become common place,
76 assembling a haploid reference is still a viable alternative to making and utilising a resource
77 intensive genome graph.

78 Reference genomes are integral parts of the analytical frameworks of genomic research.
79 Specifically, variants are identified and referred to by their loci in relation to their position
80 mapped on a reference genome. Such an approach allows for direct comparisons among
81 multiple individuals and organisms, therein enabling comprehensive research in various fields,
82 including phylogenomics (Fang et al., 2018; Wang et al., 2013), comparative evolution (Palmer

83 & Kronforst, 2020; Parker et al., 2013), adaptive radiations (Ronco et al., 2020), and the
84 genomics of domestication (Frantz et al., 2015).

85 Arguably one of the most important factors to consider when multiple reference genomes or
86 assembly versions are available is their difference in quality. Whilst we are moving towards
87 complete and error-free assemblies (Rhie et al., 2021), the continuing advances of
88 methodologies can create significant differences among assemblies. For example,
89 bioinformatic tools have been developed to resolve false gene duplications that stem from
90 heterozygosity in homologous haplotypes (Guan et al., 2020; Roach et al., 2018). In some
91 cases, such as in humans, reference genomes are continually updated alongside major
92 advances, where choosing the most updated version will offer the most accurate analysis of
93 human sequencing data (Guo et al., 2017; International Human Genome Sequencing
94 Consortium, 2001, 2004; Pushkarev et al., 2009). However, when multiple similar quality and
95 genetically diverse reference genomes are available from multiple populations or strains (e.g.,
96 Berner et al., 2019; Gan et al., 2011; Hirsch et al., 2016; Springer et al., 2018), genetic distance
97 among samples and the reference may be an important factor to consider.

98 The detection of genomic polymorphisms is affected by the evolutionary time between the
99 individuals being sequenced and the reference genome (Bohling, 2020; Prasad et al., 2022;
100 B. N. Reid et al., 2021). This has implications on both the detection and the genotyping of
101 single nucleotide polymorphisms (SNPs) and structural variants (SVs). For example, variant
102 calling through pipelines such as GATK and freebayes use Bayesian inference to call
103 genotypes (i.e., the likelihood of a genotype, given the data; Auwera et al., 2014; Garrison &
104 Marth, 2012). When high differentiation between reference genome and the sampled
105 individuals exists, a high proportion of segregating sites will emerge as fixed differences
106 between the samples and the reference genome (i.e., homozygote non-reference in diploids),
107 and therefore uncertain genotypes can have a higher likelihood of being called as homozygote
108 non-reference, even if this is not the case. Analogously, most methods used to detect SVs
109 (read-depth, split paired-read, breakpoints, and assembly) compare mapped reads to the

110 reference genome (Pirooznia et al., 2015). Several studies on humans have demonstrated
111 that ethnicity-specific reference genomes are beneficial (Ameur et al., 2017; Dewey et al.,
112 2011; Fakhro et al., 2016; Lacaze et al., 2019). Specifically, the targeted reference genomes
113 improved reliability of genetic and structural variation calls (Ameur et al., 2017; Fakhro et al.,
114 2016). Moreover, recent studies have demonstrated that increasing phylogenetic distance
115 between target species and reference genome decreases mapping efficiency and has strong
116 effects on evolutionary inferences made from the data (Bohling, 2020; Prasad et al., 2022).

117 The three-spined stickleback (*Gasterosteus aculeatus*) is a supermodel in evolutionary biology
118 (K. Reid et al., 2021), and research on this small teleost fish has pioneered discoveries related
119 to the genomics of adaptation (Feulner et al., 2015; Haenel et al., 2019; F. C. Jones et al.,
120 2012; Roesti et al., 2015), adaptive divergence (Feulner et al., 2015; Huang et al., 2016; Roesti
121 et al., 2013) and development (Shapiro et al., 2004; Spitz et al., 2001). Genomic investigations
122 using *G. aculeatus* have mostly relied on a single high-quality chromosome-level reference
123 genome from an isolated population in Alaska (F. C. Jones et al., 2012), which has been
124 updated with multiple improvements (Glazer et al., 2015; Nath et al., 2021; Peichel et al., 2017;
125 Roesti et al., 2013). Recently, several additional *de novo* *G. aculeatus* contig-level genome
126 assemblies have been made available, including European and marine derived assemblies
127 (Berner et al., 2019). These additional genome assemblies may be appropriate given the wide
128 geographic distribution of the species; there are Atlantic and Pacific clades of *G. aculeatus*
129 that diverged an estimated 44.6 Kya with extensive phenotypic and genetic diversity across
130 its range (Fang et al., 2018; McKinnon & Rundle, 2002).

131 In this study, we report the generation and *de novo* annotation of a European *G. aculeatus*
132 genome assembly derived from a gynogen individual (Samonte-Padilla et al., 2011). The
133 gynogenesis process in *G. aculeatus* produced a near complete homozygous diploid fish
134 (Samonte-Padilla et al., 2011), which helps alleviate some of the genome assembly difficulties
135 associated with heterozygosity. Then, using European and North American derived reference
136 genomes, we investigated the effect of reference genome origin. We used high-quality

137 genome-wide resequencing data from 60 *G. aculeatus* individuals from 5 recently diverged
138 lake-river pairs distributed across the European (Atlantic clade; Fang et al., 2018) and North
139 American (Western North America; Pacific clade) *G. aculeatus* ranges. The effect of using a
140 local reference genome was investigated through comparing mapping efficiency (i.e., the
141 percentage of reads that are successfully mapped to the reference genome), genotype calling,
142 genome scans for F_{ST} , Tajima's D , and π , and identification of SVs. The resequenced genome
143 data have been used to investigate the distribution of islands of differentiation across the
144 genome (Feulner et al., 2015) and the role of copy-number variation in adaptation (Chain et
145 al., 2014), offering baselines to evaluate specific metrics against a new local genome. We also
146 compared how the different genomes affect DNA-methylation calling, focusing on an
147 additional 50 European fish for which reduced-representation bisulfite sequencing (RRBS)
148 was available (Sagonas et al., 2020). We hypothesise that the mapping and genotyping results
149 will generally fall into 3 categories: (h_1) a local reference genome has a significant and
150 putatively beneficial effect, (h_2) one reference genome is better than the other, and (h_3) a local
151 reference genome has an effect, but the effects are more substantial with local populations
152 (i.e., a mixture of both h_1 and h_2). Our hypotheses can be observed in the outcome of statistical
153 tests: h_1 presents as a significant interaction between reference origin and population origin,
154 h_2 as a significant effect of reference origin, and h_3 presents similarly to h_1 with a significant
155 interaction, but the post-hoc analysis indicates a clear bias towards one of the reference
156 genomes.

157 **Material & Methods**

158 *Reference Genome Assembly and Annotation*

159 The induction of the diploid gynogen individual followed the protocol established for three-
160 spined sticklebacks (Samonte-Padilla et al., 2011). In brief, fertilised stickleback eggs were
161 mixed with UV-irradiated sperm (2 minutes of exposure) and then exposed to a heat-shock
162 treatment of 34°C for 4 minutes, 5 minutes post-fertilisation. The treatment caused the genetic

163 inactivation of the sperm, resulting in homozygote maternal offspring that lack paternal alleles
164 (Samonte-Padilla et al., 2011). In order to increase the likelihood of embryo development, two
165 siblings from the same family were used for this process. After 5 months post hatching, a fish
166 was sacrificed. DNA was extracted using the Qiagen high molecular weight extraction kit
167 following the manufacturer's protocol. Sequencing was then conducted at the Beijing
168 Genomics Institute (BGI), taking place on a PacBio platform. In total, 2,805,993 reads were
169 generated with a coverage of 44.1X. A total of 214,285 PacBio reads were discarded before
170 further analysis given their short length. In addition, Illumina paired-end sequencing libraries
171 in a HiSeq2500 platform were constructed with insert sizes of about 170 base pairs (bp), 500
172 bp and 800 bp.

173 Genome assembly was performed using Canu v1.6 assembler (Koren et al., 2017), followed
174 by an internal polishing step using Quiver. To hybrid polish the PacBio assembly, a total of
175 316,797,342 high-quality Illumina reads were mapped to the contigs using BWA-MEM v0.7.15
176 (Li, 2013) and the alignment was then used for further polishing using Pilon v1.22 (Walker et
177 al., 2014). Illumina raw reads were trimmed, and low quality and adaptor sequences were
178 removed using Cutadapt v1.13 (Martin, 2011). To evaluate the PacBio *de novo* contig-level
179 assembly and search for potential misassemblies, we used FRCbam v1.3.0 (Vezzi et al.,
180 2012), whereas its completeness in terms of core orthologous genes was assessed using
181 BUSCO v3.0.1 (Simão et al., 2015) and the 'actinopterygii' data set. The 32.1kb contig
182 tig00001189_pilon mapped to the mitochondrial genome of the North American *G. aculeatus*
183 (Peichel et al., 2017) and was trimmed and labelled the mitochondrial genome. The sequence
184 was trimmed to only include the 15.8kb that aligned to the North American mitochondrial
185 genome given the size of the mitochondrial genomes are moderately conserved even across
186 long phylogenetic distances (Gissi et al., 2008). The excess 16.3kb of contig
187 tig00001189_pilon were labelled and kept in the assembly, making up two additional contigs.
188 To scaffold the European *G. aculeatus* contig-level gynogen assembly into pseudo-
189 chromosomes we used Chromosemble from the Satsuma2 package (Grabherr et al., 2010).

190 Here, we ordered and oriented the contigs based on synteny with the North American *G.*
191 *aculeatus* chromosome-level genome (Peichel et al., 2017), excluding the unmapped
192 scaffolds. We tested for the effect of contig size on alignment rates, and only retained contigs
193 with an alignment rate of 70% or above for further assembly. Gynogen contigs not scaffolded
194 onto a pseudo-chromosome were concatenated in size order into an unmapped scaffold for
195 population genomic analyses, separating each contig by 1,000 N's. Synteny between the
196 European and North American *G. aculeatus* assemblies was calculated using the
197 SatsumaSynteny2 function (Grabherr et al., 2010), and plotted using the Circos v0.69
198 visualisation tool (Krzywinski et al., 2009). It should be noted that the reference genomes have
199 been created using distinctly different methodologies. As such, significant reference origin by
200 population origin interactions that do not clearly exhibit a reciprocal effect in the test statistic
201 likely include a genome quality effect.

202 Repetitive sequences were identified *de novo* in the European pseudo-chromosome assembly
203 using Repeat Modeler v.2.0.1 while Repeat Masker v.4.1.1 (Smit et al., 2015) was used to
204 mask the genome using the three-spined stickleback and zebrafish libraries in two separately
205 rounds. The results of each round were then analyzed together, complex repeats were
206 separated, to produce the final repeat annotation. Genome annotation was performed on the
207 European repeat-masked pseudo-chromosome genome assembly using MAKER2 v.2.31.9
208 (Holt & Yandell, 2011). Subsequent genome annotation was performed following a two-round
209 approach. For the first round, the repeat annotation data (release 95) as well as *G. aculeatus*
210 transcriptome and protein sequences from ENSEMBL and UniProt/SwissProt databases were
211 used as evidence sets for the prediction of gene models, while *est2genome* and
212 *protein2genome* setting were set as 1. For the second round, SNAP (Korf, 2004), with ADE of
213 0.25 and length of 50, and AUGUSTUS v.3.2.3 with default values (Stanke et al., 2008) were
214 trained on the gene model predicted from the first round. Functional annotation was performed
215 using BlastP against UniProt proteins with an E-value threshold of 1e-5, and InterProScan
216 v.5.4-47 (P. Jones et al., 2014) was used for domain annotation. The resulting gene models

217 were filtered to retain those with AED value of 0.5 or less, having PFAM annotations and
218 significant hits to known proteins against UniProt DB (E-value 1e-5).

219 We identified orthologous and paralogous gene families among the North American and
220 European *G. aculeatus* reference genomes using OrthoFinder v2.4.1 with the default
221 parameters (Emms & Kelly, 2019). Protein sequences were extracted using the getfasta
222 function in the BEDtools toolset v2.26.0, using the *-split* parameter to only include exonic
223 regions (Quinlan & Hall, 2010). Where applicable, downstream analyses were restricted to
224 only include the 7,529 1-to-1 orthologues identified between the two assemblies to remove
225 any biases stemming from differences in gene number or functional annotation.

226 *SNP Data Collection and Processing*

227 Whole genome resequencing data from a total of 60 *G. aculeatus* individuals were used from
228 5 recently diverged freshwater lake (_L) and river (_R) population pairs (table S1; details on
229 sampling, library preparation, sequencing, and original data processing up to adapter trimming
230 can be found in; Feulner et al., 2015). The five population pairs were sampled from two sites
231 in Germany (G1 and G2; European; Atlantic clade), and one site in Norway (No; European;
232 Atlantic clade), the United States (US; North American; Pacific clade), and Canada (Ca; North
233 American; Pacific clade).

234 For the genome scan using SNP data, raw data was processed following previous procedures
235 (Feulner et al., 2013). Adapter-cleaned reads were trimmed using Trimmomatic v0.36 (Bolger
236 et al., 2014) in paired-end mode, trimming read tails with a PHRED quality score below 20 and
237 trimming to a maximum of 50bp. Using BWA-MEM v0.7.17 (Li, 2013), reads were
238 independently mapped to both the anchored European and US reference genomes (Peichel
239 et al., 2017). Mapping efficiency was calculated using Bamtools v2.4.1 (Barnett et al., 2011).
240 All downstream processing of mapped reads and methodology for variant calling were
241 identical for both reference genomes. Mapped reads were processed using Picard toolkit
242 v2.18.7 (<https://broadinstitute.github.io/picard/>), applying FixMateInformation and CleanSam.

243 All reads belonging to the same individual from different lanes were combined using
244 MergeSamFile, and then duplicate reads were flagged using MarkDuplicates. Variant calls
245 were performed using GATK v4.0.6.1 (McKenna et al., 2010), calling variants in all genomes
246 simultaneously, split by chromosome. The final set of SNPs was produced using hard filtering
247 following the best practise workflow (see supplementary methods for filtering thresholds;
248 (Depristo et al., 2011). Genome mapping and variant calls were conducted on the QMUL
249 Apocrita High Performance Computing Cluster (King et al., 2017).

250 The gynogenesis process employed here aims to purge heterozygous variation, enabling us
251 to reconstruct complex genomic regions. To assess the proportion of the genome that remains
252 heterozygotic we used the same GATK variant calling and filtering pipeline detailed above with
253 the paired-end Illumina libraries used to polish the gynogen assembly.

254 *Phylogenetic Analyses*

255 In order to assess the phylogenetic relationship between the reference genomes and the 60
256 resequenced genomes, we compared maximum-likelihood phylogenies based on each variant
257 call with its respective reference genome. Maximum-likelihood phylogenies for both SNP calls
258 were inferred using RAxML v8.2.11 (Stamatakis, 2014). We randomly sampled 1% of all
259 segregating sites by setting the “—select-random-fraction” parameter to 0.01 in the GATK
260 function SelectVariants. The resulting VCFs were converted to PHYLIP format (Felsenstein,
261 1989) using the vcf2phylip.py script (doi:10.5281/zenodo.1257058). Trees were constructed
262 using the GTRGAMMA model with 1000 bootstraps. Phylogenetic trees were plotted using the
263 R package *ggtree* package v2.2.4 (Yu et al., 2017).

264 *Estimations of Genotype Bias*

265 Calling of genotypes (i.e., heterozygote versus homozygote) may be affected by reference
266 genome origin. Measures of genome-wide zygosity across all segregating sites were
267 performed by parsing the genotype field in the VCF file using a custom R script. Genotypes
268 were grouped into 5 distinct categories: homozygous reference, homozygous non-reference,

269 heterozygous reference/non-reference, heterozygous non-reference/non-reference, and
270 missing. This process was repeated to estimate genotypes for each individual mapped to both
271 reference genomes.

272 *Genome Scan Using SNP Data*

273 Genome scans were performed in R v4.0.2 (R Development Core Team, 2019), and
274 population genetics indices were calculated using the R package *PopGenome* v2.7.5 (Pfeifer
275 et al., 2014). We measured Tajima's D and π in each population, and F_{ST} in each parapatric
276 population pair. All metrics were calculated in non-overlapping 20kb windows across all 20
277 autosomal chromosomes and the unmapped scaffold. To obtain outlier genomic windows, we
278 extracted the top 1% of the empirical distributions for each metric and population (or population
279 pair for F_{ST}). This conservative criterion (e.g., Feulner et al., 2015; Lai et al., 2019; Stern &
280 Lee, 2020) was chosen to increase our confidence in defining outliers. Finally, we defined
281 outlier genes as any gene overlapping one or more outlier genomic windows from the SNP-
282 based genome scans using the *foverlaps* function in the R package *data.table* v1.9.6 (Dowle
283 et al., 2015).

284 *Detection of Structural Variants*

285 To investigate the impact of reference genome origin on the detection of structural variants
286 (SVs), we used two independent SV callers, DELLY2 v0.8.3 (Rausch et al., 2012) and LUMPY
287 v0.3.0 (Layer et al., 2014). Both LUMPY and DELLY were run using the default parameters.
288 The LUMPY call was genotyped using SVTyper v0.7.1 (Chiang et al., 2015), and all SVs
289 marked with the "LowQual" DELLY flag were removed. To ensure SVs found by both programs
290 were the same, only SVs with an overlap of at least 50% were accepted and merged into a
291 cohort level VCF file using SURVIVOR v1.0.3 (Jeffares et al., 2017). For downstream
292 analyses, we included autosomal duplications, deletions, and inversions with a length of
293 between 1kb and 1Mb supported by at least 6 split or discordant reads. All samples that were
294 homozygote non-reference or heterozygote across all samples were analysed separately as

295 these variants likely arise from the reference genome assemblies. Genes with coordinates
296 entirely nested within SVs were defined as structurally variable genes (SVG) using the
297 *foverlaps* function in the R package *data.table* v1.9.6.

298 *Methylation Data Processing and Genome Scan*

299 For the DNA methylation analysis, we used 50 methylomes of laboratory full-sib families of
300 European *G. aculeatus* obtained from the study of Sagonas et al. (2020), were we investigated
301 whether parasite infection alters genome-wide patterns and levels of DNA methylations. For
302 each fish, a single-end library of 100 bp reads with an average of 11.5 million reads was
303 produced. The raw data were quality checked using FASTQC v0.11.5 (Andrews, 2010).
304 Cutadapt v1.9.1 (Martin, 2011) was used to trim and filter low-quality bases (-q 20), remove
305 trimmed reads shorter than 10 bases and remove adapters using multiple adapter sequences
306 (ATCGGAAGAGCACAC, AGATCGGAAGAGCACAC and NNAGATCGGAAGAGCACAC)
307 with a minimum overlap of 1 bp between adapter and read. Trimmed reads were
308 independently mapped against the European and US reference genomes (Peichel et al.,
309 2017) to extract methylated cytosines, using Bismark v0.22.1 (Krueger & Andrews, 2011) with
310 the Bowtie2 v2.3.2 aligner, allowing up to 2 mismatches. Similar to the SNP data, Bamtools
311 v2.4.1 (Barnett et al., 2011) was used to calculate the mapping efficiency.

312 Cytosine methylation ratios in CpG sites was estimated for each fish and differentially
313 methylated sites (DMS) were calculated between the two treatment groups (no parasite
314 exposed or exposed to the nematode parasite *Camallanus lacustris*) respectively (for more
315 information, see Sagonas et al., 2020) using the R package *MethylKit* v1.14.2. CpG
316 methylation ratios were estimated by calculating the number of reads mapping to a given
317 position carrying a cytosine divided by those reads carrying either C or T. CpG sites with
318 coverage below 10X and sites that have more than 99.9th percentile of coverage were
319 discarded in each sample from downstream analyses. We selected DMS between treatments
320 using the following criteria: change in fractional methylation larger than 15%; q-values lower
321 than 0.01 (SLIM method), and presence of methylated Cs in at least 50% of the samples within

322 a treatment group. Differentially methylated genes were identified using the *genomation* R
323 package v.1.1.0 (Akalin et al., 2015); a gene was considered differentially methylated if at least
324 one DMSs was located no further than 1.5-kb upstream and 500 bases downstream of it.

325 *GO Enrichment Analysis*

326 To examine how the origin of the reference genome impacts functional enrichment of outlier
327 genes, structurally variable genes, and differentially methylated genes, we performed gene
328 ontology (GO) enrichment analyses. GO enrichment analyses were performed using the
329 g:GOST function in the g:Profiler v0.1.9 package (Raudvere et al., 2019). Outlier genes were
330 grouped by all combinations of reference genome origin versus population of origin, resulting
331 in 4 distinct combinations: Europe-Europe, Europe-North America, North America-Europe,
332 and North America-North America. The lists of outlier genes or SVGs identified using the
333 European assembly were assigned the orthologous North American gene identifiers for GO
334 enrichment. *P*-values were corrected for multiple testing using FDR.

335 *Statistical Analyses*

336 Linear mixed effect models in the *lme4* package (Bates et al., 2015) were used to analyse how
337 the origin of the reference genomes affected mapping efficiency, detection of genome-wise
338 zygosity, and population-genetic indices (i.e., Tajima's *D*, π , and F_{ST}). For mapping efficiency,
339 the proportion of mapped reads that were singletons or duplications were independently used
340 as response variables. An interaction between reference genome origin (i.e., North America
341 or Europe) and population origin (i.e., North America or Europe) were assigned as fixed
342 effects, and population ID was set as a random factor. The same approach was used for all
343 analyses, independently replacing the response variable with the zygosity categories or
344 population-genetic indices, retaining the same fixed and random effects. *P*-values were
345 inferred using Satterwaite's degree of freedom method in the *lmerTest* package (Kuznetsova
346 et al., 2017). Tukey HSD post-hoc tests were performed using *emmeans* (Lenth et al., 2020).

347 **Results**

348 *Reference Genome Assembly*

349 The contig-level European gynogen assembly is 458.4Mb, making it 1.0% smaller than the
350 North American reference genome (463.0Mb; Peichel et al., 2017). We achieved an N50 of
351 0.746Mb, comprised of 1,906 contigs (table 1). Guided by synteny, we conservatively placed
352 419.3Mb (91.5%) into 21 chromosomes (fig. 1), forming a pseudochromosome level assembly
353 allowing for a more accurate comparison of the impact of the origin of reference genomes on
354 population genomic metrics. A combination of gene evidence from the *G. aculeatus* North
355 American reference genome (available cDNA and protein sequences) and *ab initio* gene
356 predictions resulted in 22,739 genes annotated and a BUSCO completeness score of 95.2%.
357 A total of 18,255 (90.2%) genes in the European gynogen assembly were orthologous to
358 genes in the North American assembly. Additionally, we confirmed the European and North
359 American derived reference genomes are nested within the phylogeny of populations sampled
360 from the same geographic regions (supplementary fig. S1).

361 Next, we called SNPs in the paired-end libraries used to polish the European genome
362 assembly to assess the remaining heterozygosity in the gynogen genome assembly, which is
363 expected to be homozygous after the gynogenesis procedure. In total we identified 299,931
364 SNPs (average genome-wide read depth of 60.6) in the genome: 3,118 SNPs were
365 homozygote non-reference, and 296,813 were heterozygote. Hence, after two generations of
366 gynogenesis only 0.07% of the genome remains polymorphic, compared to $0.53\% \pm 0.01\%$
367 (mean \pm SE) across all samples mapped to both reference assemblies (supplementary table
368 S1). These SNPs likely stem from paralogous sequences that were not identified by the
369 genome assembler or from errors in the SNP calling process.

370 *Mapping Efficiency*

371 To assess the impact of reference genome origin on downstream analyses, we started by
372 mapping whole genome resequencing reads from 60 individuals to the reference genomes. In

373 total, we identified 10,672,162 SNPs using the North American reference genome, and
374 10,757,204 SNPs using the European reference genome (supplementary table S1). Overall,
375 we achieved an average genome-wide depth of coverage of 20.40 (range; 11.09 - 35.46) using
376 the North American reference and 20.99 (11.30 - 36.14; supplementary table S1) using the
377 European reference. Reads mapped more efficiently (i.e., a higher proportion of reads
378 mapped) to the European reference genome regardless of the population of origin with total
379 reads mapping $2.31\% \pm 0.16\%$ (European; estimate \pm SE) and $1.13\% \pm 0.20\%$ (North
380 American) more efficiently, albeit with a greater increase in efficiency for local samples (LMER;
381 Reference Origin:Population Origin, $F_{108}=21.38$, $P<0.001$; fig. 2A and supplementary table
382 S2). This same result was also observed when only considering properly matched paired-end
383 reads (i.e., paired reads where both reads map in the correct orientation; 0x2 flag), where
384 reads mapped more efficiently to the European reference, but there was a greater increase in
385 efficiency for local populations (European, $3.14\% \pm 0.22\%$; North American, $1.36\% \pm 0.27\%$;
386 Reference Origin:Population Origin, $F_{108}=25.94$, $P<0.001$; fig. 2A). There were also $0.83\% \pm$
387 0.08% (European) and $0.24\% \pm 0.09\%$ (North American) fewer singletons (i.e., where only
388 one of the paired-end reads mapped) when mapping European or North American populations
389 to the European reference (LMER; Reference Origin:Population Origin, $F_{108}=25.10$, $P<0.001$;
390 fig. 2B). Reference genome or population origin had no effect on mapping of duplicate reads
391 (LMER; Reference Origin:Population Origin, $F_{108}=0.01$, $P=0.942$; Reference Origin, $F_{108}=0.12$,
392 $P=0.729$; Population Origin, $F_8=3.76$, $P=0.088$; fig. 2B). Overall, using the European derived
393 genome assembly noticeably improved mapping efficiency irrespective of the sample origins,
394 although the effects were noticeably more efficient for European populations. Such results are
395 consistent with hypothesis h_3 , which describes that a local reference genome is beneficial, but
396 the effects are generally more substantial when using the European reference genome.

397 *Estimations of Genotype Performance*

398 When using a local reference genome, there were $6.24\% \pm 0.38\%$ (European; estimate \pm SE)
399 and $0.47\% \pm 0.47\%$ (North American) fewer missing genotypes (LMER; Reference

400 Origin:Population Origin, $F_{428}=123.97$, $P<0.001$; fig. 3 and supplementary table S2). The same
401 was true for the detection of heterozygote genotypes of both classes (i.e., heterozygote
402 reference/non-reference and non-reference/non-reference), where a local reference genome
403 decreases the number of calls by $0.13\% \pm 0.09\%$ (European) and $0.31\% \pm 0.11\%$ (North
404 American) for heterozygote reference/non-reference, and $0.10\% \pm 0.003\%$ (European) and
405 $0.05\% \pm 0.004\%$ (North American) for heterozygote non-reference/non-reference genotypes
406 (LMER; all models report the Reference Origin:Population Origin interaction; reference/non-
407 reference, $F_{428}=9.86$, $P=0.002$; non-reference/non-reference, $F_{428}=872.85$, $P<0.001$; fig. 3).
408 Conversely, we identified approximately 4 times higher proportions of homozygote reference
409 genotypes when using a local reference genome for European populations ($12.19\% \pm 0.37\%$)
410 in comparison to the North American populations ($3.36\% \pm 0.35\%$; LMER; Reference
411 Origin:Population Origin, $F_{428}=691.30$, $P<0.001$; fig. 3). Finally, approximately a two-fold
412 decrease in the proportion of homozygote non-reference variants were identified when using
413 a local reference genome for European populations ($-5.72\% \pm 0.12\%$) over the North American
414 populations ($-2.53\% \pm 0.14\%$; LMER; Reference Origin:Population Origin, $F_{428}=2012.29$,
415 $P<0.001$; fig. 3). Except for duplications which were not significantly different among calls,
416 using a local reference genome offers a benefit in the detection of every class of genotype.
417 Overall, these results are consistent with hypothesis h_1 which posited that a local reference
418 genome would offer a benefit and would manifest as significant interactions.

419 *Genome Scan Using SNP Data*

420 The genome-wide distributions of metrics commonly used in population genomics were
421 affected by the origin of the genome used (fig. 4 & S2-3). For a genome scan investigating
422 patterns of differentiation, F_{ST} was $0.019 \pm 8.4 \times 10^{-4}$ (mean \pm SE) higher for European
423 populations and $0.005 \pm 1.0 \times 10^{-5}$ higher for North American populations when using a local
424 reference genome (LMER; Reference Origin:Population Origin, $F_{220053}=324.60$, $P<0.001$;
425 supplementary table S2). A similar pattern was observed using T_D , whereby T_D was $0.026 \pm$
426 2.95×10^{-3} (European) and $5.90 \times 10^{-3} \pm 3.61 \times 10^{-3}$ (North American) higher when using a local

427 reference genome (LMER; Reference Origin:Population Origin , $F_{406709}=63.97$, $P<0.001$). In
428 addition, using a local reference genome led to significantly lower values of nucleotide diversity
429 being detected (LMER; Reference Origin:Population Origin , $F_{407698}=123.20$, $P<0.001$), with
430 low estimates for both European ($-3.28 \times 10^{-5} \pm 5.39 \times 10^{-6}$) and North American ($-9.99 \times 10^{-5} \pm$
431 6.60×10^{-6}) populations. These results are consistent with hypothesis h_1 , where a local
432 reference genome has a significant impact on analyses.

433 Through sampling each metric individually and taking the top ~1% of the F_{ST} , π , or T_D
434 distributions we generated multiple lists of outlier genes (table 2; supplementary table S3).
435 Notably, the distributions of outlier genes across the genome were not significantly different
436 when using either reference genome (two-sample Kolmogorov–Smirnov test; F_{ST} , $D=0.140$,
437 $P=0.988$; π , $D=0.121$, $P=0.998$; T_D , $D=0.157$, $P=0.962$; fig. 4 & S2-3). Overall, higher number
438 of outlier genes, including the subset of outlier 1-to-1 orthologous genes, were identified when
439 using a local reference genome (table 2). The difference in genes among calls with different
440 reference genomes putatively translated into no overlapping significantly enriched GO terms
441 for the F_{ST} , π , and T_D analyses if any enrichment was detected (table 2). Complete GO
442 enrichment tables are reported in supplementary table S4.

443 *Genomic Structural Variants*

444 We next addressed the question whether using a local reference genome affected the
445 detection of structural variants. Firstly, we generated multiple distributions of SVs organised
446 by the combination of reference genome and population origin (table 3). Overall, no fixed SVs
447 were observed in all samples. The distribution of deletions significantly differed among SV
448 calls (two-sample Kolmogorov–Smirnov test, $D=0.278$, $P=0.008$; fig. S4), whereby fewer SVs
449 were detected when using the North American reference genome. The distribution of
450 duplications and inversions did not significantly differ among SV calls with either reference
451 genome (two-sample Kolmogorov–Smirnov test; duplications, $D=0.109$, $P=0.890$; inversions,
452 $D=0.140$, $P=0.754$; fig. S4). Additionally, we identified less deletions when using a local
453 reference genome, more deletions were identified overall when using the European reference

454 genome (LMER; Reference Origin:Population Origin, $F_{108}=61.813$, $P<0.001$; table 3,
455 supplementary table S5-S6). Analogously, we identified significantly fewer inversions when
456 using a local reference genome, but more inversions were identified overall when using the
457 North American reference genome (LMER; Reference Origin:Population Origin, $F_{108}=34.52$,
458 $P<0.001$; table 3). Finally, a similar number of duplications were identified in European
459 populations irrespective of reference origin, whereas fewer duplications were identified in
460 North American populations when using a local reference genome (LMER, Reference
461 Origin:Population Origin, $F_{108}=3.99$, $P=0.048$; supplementary table S5-S6). Overall, the results
462 of the SV analysis are in line with hypothesis h_3 where the effects of a local reference genome
463 are present, but unequal effects indicate one reference is better than the other.

464 Next, we investigated the role of a local reference genome on the detection of genes entirely
465 nested within SVs, which we defined as structurally variable genes (SVG; table 3). This
466 analysis was limited to 1-to-1 orthologs to ensure there was no bias arising from copy number
467 variation among reference genome annotations. Here, we identified significantly fewer SVG-
468 deletions for European populations using a local reference genome, however there was no
469 significant difference in SVG-deletions in the North American populations when using either
470 reference (LMER, Reference Origin:Population Origin, $F_{108}=25.94$, $P<0.001$; supplementary
471 table S5-S6). On the other hand, we identified significantly more SVG-duplications when using
472 the North American reference, regardless of the origin of the population (LMER, Reference
473 Origin:Population Origin, $F_{108}=9.40$, $P=0.003$; supplementary table S5-S6). Finally,
474 significantly fewer inversions were detected when using a local reference genome (LMER;
475 Reference Origin:Population Origin, $F_{108}=62.55$, $P<0.001$; supplementary table S5-S6).

476 To identify whether a local reference genome correlated with the detection of functional
477 enrichment in SVs, we investigated the SVGs GO enrichment. Similar to the overall SVG
478 distribution analysis, this analysis was restricted to 1-to-1 orthologs. We identified no overlap
479 in functional enrichment in the majority of the comparisons (table 3). The one exception was
480 SVG-deletions in the North American populations, where 3 out of 13 significantly enriched

481 terms (signaling receptor regulator activity, signaling receptor activator activity, and receptor
482 ligand activity) were identified in both calls. Overall, the detection of SVs and SVGs were
483 affected in different ways by the origin of the reference genome.

484 *DNA Methylation Analysis*

485 Finally, we conducted a DNA methylation analysis after mapping bisulfite sequencing reads
486 to the two reference genomes. The inclusion of this analysis permits us to investigate the effect
487 of reference genome origin on both DNA methylation analyses and on marker-based analyses,
488 as opposed to the window-based genome scans reported above. The alignment of reads to
489 the references showed significantly higher efficiency when using a local European reference
490 genome (72.5%) compared to the North American reference (68.4%), resulting in an increase
491 of 6% (paired t-test; $t=-44.44$, $df=49$, $P<0.001$). The more efficient mapping to a local reference
492 produced a significantly higher calling of cytosine bases (6% increase, paired t-test; $t=-28.31$,
493 $df=49$, $P<0.001$) and methylated Cs (8.2% increase, paired t-test; $t=-33.18$, $df=49$, $P<0.001$).
494 Similarly, the comparison of the number of methylated sites per fish after filtering for low
495 coverage sites revealed that using the local European reference genome resulted in identifying
496 more methylated sites (560629.08 ± 12167.89) than with the North America reference
497 (510240.14 ± 11037.78 , paired t-test; $t=-44.20$, $df=49$, $P<0.001$). Additionally, the number of
498 Differentially Methylated Sites (DMS) was higher when using a local European reference
499 genome ($N=2550$ DMS) in comparison to the North American reference ($N=2404$ DMS). DMS
500 overlapped with 711 and 712 genes in the European and North American assemblies,
501 respectively, and specifically 298 and 299 genes were 1-to-1 orthologs between the two
502 assemblies. A total of 204 of those genes with DMS (68%) were shared in both genomes.
503 There were three significantly enriched GO terms (protein binding, calcium ion binding, and
504 binding) shared in both analyses, and two enriched GO terms (cation binding and metal ion
505 binding) only identified when using a divergent reference genome (Table 2).

506 Discussion

507 Until genome-graphs are more widely available, individual reference genomes remain an
508 integral part of population genomic analyses. However, the reference genome can introduce
509 mapping biases that significantly influence downstream analyses and inferences (Bohling,
510 2020; Prasad et al., 2022; Valiente-Mullor et al., 2021). Meanwhile, the effects of using a local
511 or more differentiated reference genome remains understudied for ecological and evolutionary
512 model species. To address this knowledge gap, we generated a *de novo* annotated synteny-
513 guided assembly of a European *Gasterosteus aculeatus* fish. Using this novel genome and
514 the established North American reference genome to map sequence data of samples from
515 different populations in Europe and North America, we confirm the reference genome origin
516 significantly impacts downstream analyses. Most notably, a local reference genome increased
517 mapping and genotyping performance. Specifically, mapping efficiency was significantly better
518 using the European reference genome, but the increase in performance was greater for local
519 samples. When using a local reference, more genomic sites were genotyped, and genome
520 window-based estimates of T_D and F_{ST} increased whilst π slightly decreased. Similarly,
521 structural variants (SVs) analysis gave slightly different results based on the reference
522 genome used. Consequently, most GO analyses resulted in only a minor proportion of
523 matching enriched GO functions when using different reference genomes. In contrast to the
524 window-based methods, the marker-based DNA methylation analysis pipeline was relatively
525 less affected by reference genome origin, but still about one third of differentially methylated
526 genes was uniquely identified by one but not both references.

527 *Genome Assembly of a Gynogenetic Individual*

528 Recent tools and techniques have increased the efficacy of reference genome assembly, such
529 as utilising long and short read sequencing (Rhie et al., 2021), scaffolding with Hi-C (Peichel
530 et al., 2017), optical or linkage mapping (Glazer et al., 2015), among the growing list of novel
531 and effective techniques (Rhie et al., 2021). The generation of gynogenetic individuals purges
532 genome-wide variation simplifying assembly of genomes (Christensen et al., 2018; Samonte-

533 Padilla et al., 2011). Here, after applying a previously established protocol for gynogenesis,
534 we putatively removed more than 99.9% of genome-wide variation, likely aiding in scaffolding
535 by long-read sequencing. The contiguity of the resulting contig-level gynogen *G. aculeatus*
536 assembly is comparable to the top few assemblies published by the Fish10k project (Fan et
537 al., 2020) in terms of number of contigs and contig N50. Notably, there are a few altered
538 placements of contigs into chromosomes among assemblies. The largest was the 2.07Mb
539 contig tig00002041_pilon, which aligns to both the middle of chrVIII (9.25Mb-10.87Mb) and
540 the end of chrIX (17.89Mb-18.29Mb) and was placed in Gy_chrIX by Chromosome. The
541 Atlantic and Pacific *G. aculeatus* clades diverged an estimated 44.6Kya (Fang et al., 2018)
542 leaving substantial time for large genomic rearrangements to occur. As such the correct
543 placement of tig00002041_pilon is similarly likely in either chromosome which illustrates the
544 need for further investigations to resolve the differences among assemblies. Overall, the new
545 European gynogen reference genome is high quality, enabling us to test the effects of
546 reference genome origin on downstream population genomic analyses.

547 *Mapping and Calling Variants*

548 Despite continuing advances in tools to assemble reference genomes and map sequenced
549 reads, difficulty remains in correctly mapping reads to complex genomic regions enriched in
550 heterozygosity, structural variation, or repetitive elements (Kajitani et al., 2014; Treangen &
551 Salzberg, 2012). By using a reference genome with a longer evolutionary time to the most
552 recent common ancestor (MRCA), complex variants have time to accumulate, likely
553 decreasing mapping efficiency to genomic regions with arguably some of the most sought-
554 after features (e.g., polymorphic regions associated with rapid evolutionary changes and
555 adaptations). Here, we show that using a European stickleback reference genome that has a
556 lower time to the MRCA with European populations increases mapping efficiency and
557 decreases missing data. Conversely, the North American populations also showed increased
558 efficiency when mapped to the European reference, but the difference was noticeably smaller
559 than for European populations. Such a result indicates the removal of heterozygosity through

560 gynogenesis (Samonte-Padilla et al., 2011) and the putative resolution of complex genomic
561 regions in the European assembly improved mapping efficiency. These results are concordant
562 with ethnicity-specific reference genome studies, which have demonstrated that local
563 reference genomes increase depth of coverage resulting in increased sensitivity in variant
564 calling (Ameur et al., 2017; Dewey et al., 2011; Fakhro et al., 2016).

565 ***Genome Scans***

566 The effects of improved mapping efficiency and a decrease in missing data were observed to
567 have significant impacts on the estimation of important population genomic metrics. Here,
568 genome-wide estimates of F_{ST} and T_D were higher when using a local reference genome,
569 whereas the opposite pattern was true for estimates of nucleotide diversity (π). Despite the
570 differences in genome-wide estimates, the genome-wide distribution of outlier windows of π ,
571 F_{ST} , and T_D did not significantly differ across the genome for the same resequenced
572 populations mapped to different reference genomes. Crucially, however, the detection of
573 outlier genes was strongly impacted when using different reference genomes, even when
574 conservatively limiting the analysis to 1-to-1 orthologs identified among the references.
575 Specifically, genes overlapping π outliers had a low proportion of matching orthologs in the
576 same populations when mapped to different reference genomes. Genes overlapping outliers
577 from scans for F_{ST} and T_D were more consistent, but still revealed a large number of
578 differences. In total, only 5.45% of the orthologs among assemblies were mapped to different
579 chromosomes, clearly affecting the detection of outlier genes but only explaining a small
580 proportion of differences observed. The difference in gene placement may instead highlight
581 numerous resolved differences among assemblies that have accumulated since the
582 divergence of Atlantic and Pacific *G. aculeatus* clades 44.6 Kya (Fang et al., 2018). For
583 example, a small deletion in one reference assembly and not the other can result in a gene
584 overlapping an outlier genomic window in only one scan. Overall improved mapping may help
585 specific population genomic analyses including genome-wide representation sequencing

586 where population structure may end up obscuring some SNPs present in only one or few
587 populations (e.g., Baltazar-Soares et al., 2020).

588 *Structural Variant Detection*

589 Similar to the effect of reference genome origin on SNP-based scans, the detection of SVs
590 appears to be affected by both reference genome origin and the assembly regardless of origin.
591 Firstly, fewer deletions and inversions were identified when using a local reference genome.
592 This result follows expectations, as there is less time between MRCA for SVs to build up
593 between the sampled population and the reference genome. Secondly, more deletions and
594 duplications and fewer inversions were detected when using the European reference,
595 irrespective of population origin, suggesting differences in the genome assembly plays a role
596 in the detection of SVs. However, the differences in SV detection did not translate into any
597 significant differences in the number of genes overlapping deletions. Overall, our results
598 suggest the detection of SVs may be affected by a combination of mapping efficiency, time to
599 MCRA, and the methods used to assemble a reference genome.

600 *Methylation*

601 The most consistent analysis in terms of overlap among reference genomes was the marker-
602 based DNA methylation test. Firstly, using a local reference genome significantly increased
603 mapping efficiency, which resulted in more methylated sites and DMS being detected. The
604 number of genes overlapping the DMS using either reference genomes was the most
605 consistent among all analyses, with one fewer gene (0.14% of total genes) and ortholog
606 (0.34% of total 1-to-1 orthologs) being identified when using a local reference. The DMS
607 analyses recovered a relatively high proportion of overlapping outlier orthologs among
608 reference genomes (68% of 1-to-1 orthologs), but still revealed an effect of the choice of
609 reference. The higher proportion of overlap compared to window-based analyses may be due
610 to the marker-based approach, which is less sensitive to genomic translocation, genome
611 evolution, or assembly errors.

612 *GO Enrichment*

613 The largest effect of reference genome origin was in the GO enrichment analyses of outlier
614 genes from genome scans, with only a minor proportion of enriched GO terms overlapping
615 when using different reference genomes. Given the overall small proportion of overlapping
616 outlier genes, these results were to be expected. GO enrichment analyses are particularly
617 sensitive to minor changes in the number of genes or annotations in lists of genes (Gaudet &
618 Dessimoz, 2017). It should be noted, however, that to allow for a direct comparison of the
619 effects of the different reference genomes, we focused on 1-to-1 orthologs. GO enrichment
620 analyses are common in population genomics (e.g., Chain et al., 2014; Feulner et al., 2015;
621 Reimegård et al., 2017; Liu et al., 2018), and our results highlight reference genome origin
622 strongly impacts such inferences.

623 *Conclusions*

624 Assembling reference genomes is a fast-moving field of research, which sees persistent
625 updates and novel methodologies adopted (Rhie et al., 2021). Hence, variation seen in new
626 reference genomes can reflect both the geographical range of the species distribution but also
627 variation in methodologies used to sequence and assemble the genomes. For example, the
628 two *G. aculeatus* genomes used here originate from samples representing two distinct
629 lineages, the European and North American lineage but also differ significantly in how they
630 were generated. Notably, the North American reference genome (Peichel et al., 2017) is part
631 of a series of updates to the original *G. aculeatus* genome assembly (F. C. Jones et al., 2012).
632 The original assembly used entirely Sanger sequence data (F. C. Jones et al., 2012),
633 compared to the PacBio and Illumina sequence data used for the gynogen genome. As such,
634 only when there is a significant interaction between population and reference origin and no
635 obvious bias in the observations towards either reference can we exclude that the differences
636 in sequencing and assembly methodologies are not the primary cause for the observed
637 patterns.

638 The aim of this study was to investigate the effects of a local reference genome and its effects
639 on downstream analyses. The reference-specific patterns of our results highlight that there is
640 no simple solution. We suggest that the quality of the reference genome and annotations
641 remains the single most important factor when choosing which reference to use. However,
642 when multiple similar quality references are available, a local reference genome offers higher
643 mapping efficiencies and decreases the proportion of missing data. The smallest reference
644 effect among our analyses was for the marker-based methylation analysis, which had
645 markedly more overlap among outliers in comparison to the window-based approach or the
646 SV analysis, but still had over 30% of outliers that did not overlap. Taken together, using a
647 local reference genome should increase the confidence of inferences made within a study,
648 even if the difference is only minor.

649 *Data Accessibility and Benefit-Sharing*

650 The raw genomic sequences of the 60 *G. aculeatus* fish were obtained from previous
651 publications (Chain et al., 2014; Feulner et al., 2015), and retrieved from the European
652 Nucleotide Archive, accession number ERP004574. The raw methylome sequences were
653 obtained from a previous publication (Sagonas et al., 2020), retrieved from the NIH genetic
654 sequence database, accession number PRJNA605637.

655 The European-derived gynogen reference genome assembly and their annotations are
656 available from the European Nucleotide Archive (ENA) accession number PRJEB54679.
657 Please note, to comply with ENA submission guidelines the unmapped chromosome (chrUn)
658 was broken into individual contigs, and annotations were lifted over using a custom R script.
659 A total of 316 gene annotations spanned contig boundaries in chrUn and were removed. The
660 original chrUn sequence and annotations are available upon request.

661 Scripts used in the data preparation and analysis pipelines are available online
662 (https://github.com/dthorburn/Origin_Matters).

663 *Acknowledgements*

664 We thank Katie Peichel and Richard Nichols for their useful comments and discussion. We
665 also thank Queen Mary University of London ITS Research support for technical assistance.

666 *Author Contributions*

667 D.M.J.T. and C.E. conceived and designed the study. F.J.J.C., P.G.D.F., C.E., T.L.L., M.B.P.,
668 and I.E.S.P. obtained the samples and oversaw the sequencing. T.B.H.R., E.B.B. and M.M.
669 created the Big Screen Consortium with grant support from the Max Planck Society to M.M.
670 K.S. and M.B.P. oversaw the initial genome assembly and annotation. D.M.J.T. analysed the
671 data, advised by C.E. D.M.J.T. and C.E. drafted the manuscript. All co-authors contributed to
672 the final version of the manuscript. C.E. acknowledges the support of the German Science
673 Foundation (DFG, EI841/4-1 and EI 841/6-1). D.M.J.T. was supported by a studentship from
674 Queen Mary University of London.

675 *References*

676 Akalin, A., Franke, V., Vlahoviček, K., Mason, C. E., & Schübeler, D. (2015). Genomation: A
677 toolkit to summarize, annotate and visualize genomic intervals. *Bioinformatics*, 31(7),
678 1127–1129. <https://doi.org/10.1093/bioinformatics/btu775>

679 Ameur, A., Dahlberg, J., Olason, P., Vezzi, F., Karlsson, R., Martin, M., Viklund, J., Kähäri,
680 A. K., Lundin, P., Che, H., Thutkaworapin, J., Eisfeldt, J., Lampa, S., Dahlberg, M.,
681 Hagberg, J., Jareborg, N., Liljedahl, U., Jonasson, I., Johansson, Å., ... Gyllensten, U.
682 (2017). SweGen: A whole-genome data resource of genetic variability in a cross-
683 section of the Swedish population. *European Journal of Human Genetics*, 25(11),
684 1253–1260. <https://doi.org/10.1038/ejhg.2017.130>

685 Andrews, S. (2010). FASTQC A Quality Control tool for High Throughput Sequence Data.
686 *Babraham Institute*.

687 Auwera, G. A. van der, Carneiro, M. O., Chris Hartl, R. P., Angel, G. del, Levy-Moonshine,
688 A., Jordan, T., Shakir, K., Roazen, D., Thibault, J., Banks, E., Garimella1, K. v.,
689 Altshuler, D., Gabriel, S., & DePristo, M. A. (2014). From FastQ data to high confidence
690 variant calls: the Genome Analysis Toolkit best practices pipeline. *Current Protocols in
691 Bioinformatics*.

692 Baltazar-Soares, M., Klein, J. D., Correia, S. M., Reischig, T., Taxonera, A., Roque, S. M.,
693 dos Passos, L., Durão, J., Lomba, J. P., Dinis, H., Cameron, S. J. K., Stiebens, V. A., &
694 Eizaguirre, C. (2020). Distribution of genetic diversity reveals colonization patterns and
695 philopatry of the loggerhead sea turtles across geographic scales. *Scientific Reports*,
696 10(1). <https://doi.org/10.1038/s41598-020-74141-6>

697 Barnett, D. W., Garrison, E. K., Quinlan, A. R., St̄mberg, M. P., & Marth, G. T. (2011).
698 Bamtools: A C++ API and toolkit for analyzing and managing BAM files. *Bioinformatics*,
699 27(12), 1691–1692. <https://doi.org/10.1093/bioinformatics/btr174>

700 Bates, D., Mächler, M., Bolker, B. M., & Walker, S. C. (2015). Fitting linear mixed-effects
701 models using lme4. *Journal of Statistical Software*, 67(1), 1–48.
702 <https://doi.org/10.18637/jss.v067.i01>

703 Berner, D., Roesti, M., Bilobram, S., Chan, S. K., Kirk, H., Pandoh, P., Taylor, G. A., Zhao,
704 Y., Jones, S. J. M., & Defaveri, J. (2019). De novo sequencing, assembly, and
705 annotation of four threespine stickleback genomes based on microfluidic partitioned
706 DNA libraries. *Genes*, 10(6), 10–15. <https://doi.org/10.3390/genes10060426>

707 Bohling, J. (2020). Evaluating the effect of reference genome divergence on the analysis of
708 empirical RADseq datasets. *Ecology and Evolution*, 10(14), 7585–7601.
709 <https://doi.org/10.1002/ece3.6483>

710 Bolger, A. M., Lohse, M., & Usadel, B. (2014). Trimmomatic: A flexible trimmer for Illumina
711 sequence data. *Bioinformatics*, 30(15), 2114–2120.
712 <https://doi.org/10.1093/bioinformatics/btu170>

713 Chain, F. J. J., Feulner, P. G. D., Panchal, M., Eizaguirre, C., Samonte, I. E., Kalbe, M.,
714 Lenz, T. L., Stoll, M., Bornberg-Bauer, E., Milinski, M., & Reusch, T. B. H. (2014).
715 Extensive Copy-Number Variation of Young Genes across Stickleback Populations.
716 *PLoS Genetics*, 10(12), 1–18. <https://doi.org/10.1371/journal.pgen.1004830>

717 Chiang, C., Layer, R. M., Faust, G. G., Lindberg, M. R., Rose, D. B., Garrison, E. P., Marth,
718 G. T., Quinlan, A. R., & Hall, I. M. (2015). SpeedSeq: Ultra-fast personal genome
719 analysis and interpretation. *Nature Methods*, 12(10), 966–968.
720 <https://doi.org/10.1038/nmeth.3505>

721 Christensen, K. A., Leong, J. S., Sakhrai, D., Biagi, C. A., Minkley, D. R., Withler, R. E.,
722 Rondeau, E. B., Koop, B. F., & Devlin, R. H. (2018). Chinook salmon (*Oncorhynchus*
723 *tshawytscha*) genome and transcriptome. *PLoS ONE*, 13(4), 1–15.
724 <https://doi.org/10.1371/journal.pone.0195461>

725 Depristo, M. A., Banks, E., Poplin, R., Garimella, K. v., Maguire, J. R., Hartl, C., Philippakis,
726 A. A., del Angel, G., Rivas, M. A., Hanna, M., McKenna, A., Fennell, T. J., Kurnytsky, A.
727 M., Sivachenko, A. Y., Cibulskis, K., Gabriel, S. B., Altshuler, D., & Daly, M. J. (2011). A
728 framework for variation discovery and genotyping using next-generation DNA
729 sequencing data. *Nature Genetics*, 43(5), 491–501. <https://doi.org/10.1038/ng.806>

730 Dewey, F. E., Chen, R., Cordero, S. P., Ormond, K. E., Caleshu, C., Karczewski, K. J.,
731 Whirl-Carrillo, M., Wheeler, M. T., Dudley, J. T., Byrnes, J. K., Cornejo, O. E., Knowles,
732 J. W., Woon, M., Sangkuhl, K., Gong, L., Thorn, C. F., Hebert, J. M., Capriotti, E.,
733 David, S. P., ... Ashley, E. A. (2011). Phased whole-genome genetic risk in a family
734 quartet using a major allele reference sequence. *PLoS Genetics*, 7(9).
735 <https://doi.org/10.1371/journal.pgen.1002280>

736 Dowle, M., Srinivasan, A., Short, T., Lianoglou, S., Saporta, R., & Antonyan, E. (2015).
737 *data.table: extension of data.frame. R package version 1.9.6.* <https://cran.r-project.org/package=data.table>

739 Emms, D. M., & Kelly, S. (2019). OrthoFinder: Phylogenetic orthology inference for
740 comparative genomics. *Genome Biology*, 20(238), 1–14.
741 <https://doi.org/10.1101/466201>

742 Fakhro, K. A., Staudt, M. R., Ramstetter, M. D., Robay, A., Malek, J. A., Badii, R., Al-Marri,
743 A. A. N., Khalil, C. A., Al-Shakaki, A., Chidiac, O., Stadler, D., Zirie, M., Jayyousi, A.,
744 Salit, J., Mezey, J. G., Crystal, R. G., & Rodriguez-Flores, J. L. (2016). The Qatar
745 genome: A population-specific tool for precision medicine in the Middle East. *Human
746 Genome Variation*, 3(August 2015), 1–7. <https://doi.org/10.1038/hgv.2016.16>

747 Fan, G., Song, Y., Yang, L., Huang, X., Zhang, S., Zhang, M., Yang, X., Chang, Y., Zhang,
748 H., Li, Y., Liu, S., Yu, L., Chu, J., Seim, I., Feng, C., Near, T. J., Wing, R. A., Wang, W.,
749 Wang, K., ... He, S. (2020). Initial data release and announcement of the 10,000 Fish
750 Genomes Project (Fish10K). *GigaScience*, 9(8), 1–7.
751 <https://doi.org/10.1093/gigascience/giaa080>

752 Fang, B., Merilä, J., Ribeiro, F., Alexandre, C. M., & Momigliano, P. (2018). Molecular
753 Phylogenetics and Evolution Worldwide phylogeny of three-spined sticklebacks.
754 *Molecular Phylogenetics and Evolution*, 127(June), 613–625.
755 <https://doi.org/10.1016/j.ympev.2018.06.008>

756 Felsenstein, J. (1989). PHYLIP—Phylogeny Inference Package (version 3.2). *Cladistics*, 5,
757 164–166.

758 Feulner, P. G. D., Chain, F. J. J., Panchal, M., Eizaguirre, C., Kalbe, M., Lenz, T. L., Mundry,
759 M., Samonte, I. E., Stoll, M., Milinski, M., Reusch, T. B. H., & Bornberg-Bauer, E.
760 (2013). Genome-wide patterns of standing genetic variation in a marine population of
761 three-spined sticklebacks. *Molecular Ecology*, 22(3), 635–649.
762 <https://doi.org/10.1111/j.1365-294X.2012.05680.x>

763 Feulner, P. G. D., Chain, F. J. J., Panchal, M., Huang, Y., Eizaguirre, C., Kalbe, M., Lenz, T.
764 L., Samonte, I. E., Stoll, M., Bornberg-Bauer, E., Reusch, T. B. H., & Milinski, M.
765 (2015). Genomics of Divergence along a Continuum of Parapatric Population
766 Differentiation. *PLoS Genetics*, 11(2), 1–18.
767 <https://doi.org/10.1371/journal.pgen.1004966>

768 Formenti, G., Theissinger, K., Fernandes, C., Bista, I., Bombarely, A., Bleidorn, C., Ciofi, C.,
769 Crottini, A., Godoy, J. A., Höglund, J., Malukiewicz, J., Mouton, A., Oomen, R. A., Paez,
770 S., Palsbøll, P. J., Pampoulie, C., Ruiz-López, M. J., Svardal, H., Theofanopoulou, C., ...
771 Zammit, G. (2022). The era of reference genomes in conservation genomics. *Trends
772 in Ecology and Evolution*, 37(3), 197–202. <https://doi.org/10.1016/j.tree.2021.11.008>

773 Frantz, L. A. F., Schraiber, J. G., Madsen, O., Megens, H. J., Cagan, A., Bosse, M., Paudel,
774 Y., Crooijmans, R. P. M. A., Larson, G., & Groenen, M. A. M. (2015). Evidence of long-
775 term gene flow and selection during domestication from analyses of Eurasian wild and
776 domestic pig genomes. *Nature Genetics*, 47(10), 1141–1148.
777 <https://doi.org/10.1038/ng.3394>

778 Gan, X., Stegle, O., Behr, J., Steffen, J. G., Drewe, P., Hildebrand, K. L., Lyngsoe, R.,
779 Schultheiss, S. J., Osborne, E. J., Sreedharan, V. T., Kahles, A., Bohnert, R., Jean, G.,
780 Derwent, P., Kersey, P., Belfield, E. J., Harberd, N. P., Kemen, E., Toomajian, C., ...
781 Mott, R. (2011). Multiple reference genomes and transcriptomes for *Arabidopsis
782 thaliana*. *Nature*, 477(7365), 419–423. <https://doi.org/10.1038/nature10414>

783 Garrison, E., & Marth, G. (2012). *Haplotype-based variant detection from short-read*
784 *sequencing*. 1–9. <http://arxiv.org/abs/1207.3907>

785 Gaudet, P., & Dessimoz, C. (2017). *Gene ontology: pitfalls, biases, and remedies* (C.
786 Dessimoz & N. Škunca, Eds.). Humana Press. https://doi.org/10.1007/978-1-4939-3743-1_14

788 Gissi, C., Iannelli, F., & Pesole, G. (2008). Evolution of the mitochondrial genome of
789 Metazoa as exemplified by comparison of congeneric species. *Heredity*, 101(4), 301–
790 320. <https://doi.org/10.1038/hdy.2008.62>

791 Glazer, A. M., Killingbeck, E. E., Mitros, T., Rokhsar, D. S., & Miller, C. T. (2015). Genome
792 assembly improvement and mapping convergently evolved skeletal traits in
793 sticklebacks with genotyping-by-sequencing. *G3: Genes, Genomes, Genetics*, 5(7),
794 1463–1472. <https://doi.org/10.1534/g3.115.017905>

795 Grabherr, M. G., Russell, P., Meyer, M., Mauceli, E., Alföldi, J., di Palma, F., & Lindblad-Toh,
796 K. (2010). Genome-wide synteny through highly sensitive sequence alignment:
797 Satsuma. *Bioinformatics*. <https://doi.org/10.1093/bioinformatics/btq102>

798 Grytten, I., Rand, K. D., Nederbragt, A. J., & Sandve, G. K. (2020). Assessing graph-based
799 read mappers against a baseline approach highlights strengths and weaknesses of
800 current methods. *BMC Genomics*, 21(1), 1–9. <https://doi.org/10.1186/s12864-020-6685-y>

802 Guan, D., Guan, D., McCarthy, S. A., Wood, J., Howe, K., Wang, Y., Durbin, R., & Durbin, R.
803 (2020). Identifying and removing haplotypic duplication in primary genome assemblies.
804 *Bioinformatics*, 36(9), 2896–2898. <https://doi.org/10.1093/bioinformatics/btaa025>

805 Guo, Y., Dai, Y., Yu, H., Zhao, S., Samuels, D. C., & Shyr, Y. (2017). Improvements and
806 impacts of GRCh38 human reference on high throughput sequencing data analysis.
807 *Genomics*, 109(2), 83–90. <https://doi.org/10.1016/j.ygeno.2017.01.005>

808 Haenel, Q., Roesti, M., Moser, D., MacColl, A. D. C., & Berner, D. (2019). Predictable
809 genome-wide sorting of standing genetic variation during parallel adaptation to basic
810 versus acidic environments in stickleback fish. *Evolution Letters*, 3(1), 28–42.
811 <https://doi.org/10.1002/evl3.99>

812 Hirsch, C. N., Hirsch, C. D., Brohammer, A. B., Bowman, M. J., Soifer, I., Barad, O., Shem-
813 Tov, D., Baruch, K., Lu, F., Hernandez, A. G., Fields, C. J., Wright, C. L., Koehler, K.,
814 Springer, N. M., Buckler, E., Buell, C. R., de Leon, N., Kaeppler, S. M., Childs, K. L., &
815 Mikel, M. A. (2016). Draft assembly of elite inbred line PH207 provides insights into
816 genomic and transcriptome diversity in maize. *Plant Cell*, 28(11), 2700–2714.
817 <https://doi.org/10.1105/tpc.16.00353>

818 Holt, C., & Yandell, M. (2011). MAKER2: An annotation pipeline and genome-database
819 management tool for second-generation genome projects. *BMC Bioinformatics*, 12(1).
820 <https://doi.org/10.1186/1471-2105-12-491>

821 Huang, Y., Chain, F. J. J., Panchal, M., Eizaguirre, C., Kalbe, M., Lenz, T. L., Samonte, I. E.,
822 Stoll, M., Bornberg-Bauer, E., Reusch, T. B. H., Milinski, M., & Feulner, P. G. D. (2016).
823 Transcriptome profiling of immune tissues reveals habitat-specific gene expression
824 between lake and river sticklebacks. *Molecular Ecology*, 25(4), 943–958.
825 <https://doi.org/10.1111/mec.13520>

826 International Human Genome Sequencing Consortium. (2001). Initial sequencing and
827 analysis of the human genome. *Nature*, 409(6822), 860–921.
828 <https://doi.org/10.1038/35057062>

829 International Human Genome Sequencing Consortium. (2004). Finishing the euchromatic
830 sequence of the human genome. *Nature*, 431(7011), 931–945.

831 Jeffares, D. C., Jolly, C., Hoti, M., Speed, D., Shaw, L., Rallis, C., Balloux, F., Dessimoz, C.,
832 Bähler, J., & Sedlazeck, F. J. (2017). Transient structural variations have strong effects
833 on quantitative traits and reproductive isolation in fission yeast. *Nature Communications*, 8(14061), 1–11. <https://doi.org/10.1038/ncomms14061>

835 Jones, F. C., Grabherr, M. G., Chan, Y. F., Russell, P., Mauceli, E., Johnson, J., Swofford,
836 R., Pirun, M., Zody, M. C., White, S., Birney, E., Searle, S., Schmutz, J., Grimwood, J.,
837 Dickson, M. C., Myers, R. M., Miller, C. T., Summers, B. R., Knecht, A. K., ... Kingsley,
838 D. M. (2012). The genomic basis of adaptive evolution in threespine sticklebacks.
839 *Nature*, 484(7392), 55–61. <https://doi.org/10.1038/nature10944>

840 Jones, M. R., & Good, J. M. (2016). Targeted capture in evolutionary and ecological
841 genomics. *Molecular Ecology*, 25(1), 185–202. <https://doi.org/10.1111/mec.13304>

842 Jones, P., Binns, D., Chang, H. Y., Fraser, M., Li, W., McAnulla, C., McWilliam, H., Maslen,
843 J., Mitchell, A., Nuka, G., Pesseat, S., Quinn, A. F., Sangrador-Vegas, A.,
844 Scheremetjew, M., Yong, S. Y., Lopez, R., & Hunter, S. (2014). InterProScan 5:
845 Genome-scale protein function classification. *Bioinformatics*, 30(9), 1236–1240.
846 <https://doi.org/10.1093/bioinformatics/btu031>

847 Kajitani, R., Toshimoto, K., Noguchi, H., Toyoda, A., Ogura, Y., Okuno, M., Yabana, M.,
848 Harada, M., Nagayasu, E., Maruyama, H., Kohara, Y., Fujiyama, A., Hayashi, T., & Itoh,
849 T. (2014). Efficient de novo assembly of highly heterozygous genomes from whole-
850 genome shotgun short reads. *Genome Research*, 24(8), 1384–1395.
851 <https://doi.org/10.1101/gr.170720.113>

852 Kao, R. R., Haydon, D. T., Lycett, S. J., & Murcia, P. R. (2014). Supersize me: How whole-
853 genome sequencing and big data are transforming epidemiology. *Trends in
854 Microbiology*, 22(5), 282–291. <https://doi.org/10.1016/j.tim.2014.02.011>

855 Kim, D., Paggi, J. M., Park, C., Bennett, C., & Salzberg, S. L. (2019). Graph-based genome
856 alignment and genotyping with HISAT2 and HISAT-genotype. *Nature Biotechnology*,
857 37(8), 907–915. <https://doi.org/10.1038/s41587-019-0201-4>

858 King, T., Butcher, S., & Zalewski, L. (2017). *Apocrita - High Performance Computing Cluster
859 For Queen Mary University Of London*. <https://doi.org/10.5281/ZENODO.438045>

860 Koren, S., Walenz, B. P., Berlin, K., Miller, J. R., Bergman, N. H., & Phillippy, A. M. (2017).
861 Canu: Scalable and accurate long-read assembly via adaptive κ -mer weighting and
862 repeat separation. *Genome Research*, 27(5), 722–736.
863 <https://doi.org/10.1101/gr.215087.116>

864 Korf, I. (2004). Gene finding in novel genomes. *BMC Bioinformatics*, 5, 1–9.
865 <https://doi.org/10.1186/1471-2105-5-59>

866 Krueger, F., & Andrews, S. R. (2011). Bismark: A flexible aligner and methylation caller for
867 Bisulfite-Seq applications. *Bioinformatics*, 27(11), 1571–1572.
868 <https://doi.org/10.1093/bioinformatics/btr167>

869 Krzywinski, M., Schein, J., Birol, I., Connors, J., Gascoyne, R., Horsman, D., Jones, S. J., &
870 Marra, M. A. (2009). Circos: An information aesthetic for comparative genomics.
871 *Genome Research*. <https://doi.org/10.1101/gr.092759.109>

872 Kuznetsova, A., Brockhoff, P. B., & Christensen, R. H. B. (2017). lmerTest Package: Tests in
873 Linear Mixed Effects Models. *Journal of Statistical Software*, 82(13), 1–26.
874 <https://doi.org/10.18637/jss.v082.i13>

875 Lacaze, P., Pinesi, M., Kaplan, W., Stone, A., Brion, M. J., Woods, R. L., McNamara, M.,
876 McNeil, J. J., Dinger, M. E., & Thomas, D. M. (2019). The Medical Genome Reference
877 Bank: a whole-genome data resource of 4000 healthy elderly individuals. Rationale and
878 cohort design. *European Journal of Human Genetics*, 27(2), 308–316.
879 <https://doi.org/10.1038/s41431-018-0279-z>

880 Lai, Y. T., Yeung, C. K. L., Omland, K. E., Pang, E. L., Hao, Y., Liao, B. Y., Cao, H. F.,
881 Zhang, B. W., Yeh, C. F., Hung, C. M., Hung, H. Y., Yang, M. Y., Liang, W., Hsu, Y. C.,
882 Yao, C. te, Dong, L., Lin, K., & Li, S. H. (2019). Standing genetic variation as the
883 predominant source for adaptation of a songbird. *Proceedings of the National Academy
884 of Sciences of the United States of America*. <https://doi.org/10.1073/pnas.1813597116>

885 Lappalainen, I., Lopez, J., Skipper, L., Heffernon, T., Spalding, J. D., Garner, J., Chen, C.,
886 Maguire, M., Corbett, M., Zhou, G., Paschall, J., Ananiev, V., Flicek, P., & Church, D.
887 M. (2013). DbVar and DGVa: Public archives for genomic structural variation. *Nucleic
888 Acids Research*, 41, 936–941. <https://doi.org/10.1093/nar/gks1213>

889 Layer, R. M., Chiang, C., Quinlan, A. R., & Hall, I. M. (2014). LUMPY: A probabilistic
890 framework for structural variant discovery. *Genome Biology*, 15(6), 1–19.
891 <https://doi.org/10.1186/gb-2014-15-6-r84>

892 Lenth, R., Singmann, H., Love, J., Buerkner, P., & Herve, M. (2020). emmeans : Estimated
893 Marginal Means, aka Least-Squares Means. In *R package version 1.15-15*.
894 [https://doi.org/10.1080/00031305.1980.10483031>.License](https://doi.org/10.1080/00031305.1980.10483031)

895 Li, H. (2013). Aligning sequence reads, clone sequences and assembly contigs with BWA-
896 MEM. *ArXiv*, 1–3. <http://arxiv.org/abs/1303.3997>

897 Liu, D., Hunt, M., & Tsai, I. J. (2018). Inferring synteny between genome assemblies: A
898 systematic evaluation. *BMC Bioinformatics*, 19(1), 1–13.
899 <https://doi.org/10.1186/s12859-018-2026-4>

900 Martin, M. (2011). Cutadapt removes adapter sequences from high-throughput sequencing
901 reads. *EMBnet.Journal*, 17(1), 1–3.

902 McKenna, A., Hanna, M., Banks, E., Sivachenko, A., Cibulskis, K., Kernytsky, A., Garimella,
903 K., Altshuler, D., Gabriel, S., Daly, M., & DePristo, M. A. (2010). The genome analysis
904 toolkit: A MapReduce framework for analyzing next-generation DNA sequencing data.
905 *Genome Research*, 20(9), 1297–1303. <https://doi.org/10.1101/gr.107524.110>

906 Nath, S., Shaw, D. E., & White, M. A. (2021). Improved contiguity of the threespine
907 stickleback genome using long-read sequencing. *G3 Genes/Genomes/Genetics*, 0(0),
908 1–9. <https://doi.org/10.1093/g3journal/jkab007>

909 Palmer, D. H., & Kronforst, M. R. (2020). A shared genetic basis of mimicry across
910 swallowtail butterflies points to ancestral co-option of doublesex. *Nature
911 Communications*, 11(1), 1–10. <https://doi.org/10.1038/s41467-019-13859-y>

912 Parker, J., Tsagkogeorga, G., Cotton, J. A., Liu, Y., Provero, P., Stupka, E., & Rossiter, S. J.
913 (2013). Genome-wide signatures of convergent evolution in echolocating mammals.
914 *Nature*, 502(7470), 228–231. <https://doi.org/10.1038/nature12511>

915 Peichel, C. L., Sullivan, S. T., Liachko, I., & White, M. A. (2017). Improvement of the
916 Threespine Stickleback Genome Using a Hi-C-Based Proximity-Guided Assembly.
917 *Journal of Heredity*, 108(6), 693–700. <https://doi.org/10.1093/jhered/esx058>

918 Pfeifer, B., Wittelsbürger, U., Ramos-Onsins, S. E., & Lercher, M. J. (2014). PopGenome: An
919 efficient swiss army knife for population genomic analyses in R. *Molecular Biology and*
920 *Evolution*, 31(7), 1929–1936. <https://doi.org/10.1093/molbev/msu136>

921 Pirooznia, M., Goes, F., & Zandi, P. P. (2015). Whole-genome CNV analysis: Advances in
922 computational approaches. *Frontiers in Genetics*, 6(MAR), 1–9.
923 <https://doi.org/10.3389/fgene.2015.00138>

924 Prasad, A., Lorenzen, E. D., & Westbury, M. v. (2022). Evaluating the role of reference-
925 genome phylogenetic distance on evolutionary inference. *Molecular Ecology*
926 *Resources*, 22(1), 45–55. <https://doi.org/10.1111/1755-0998.13457>

927 Pritt, J., Chen, N. C., & Langmead, B. (2018). FORGe: Prioritizing variants for graph
928 genomes 06 Biological Sciences 0604 Genetics. *Genome Biology*, 19(1), 1–16.
929 <https://doi.org/10.1186/s13059-018-1595-x>

930 Pushkarev, D., Neff, N. F., & Quake, S. R. (2009). Single-molecule sequencing of an
931 individual human genome. *Nature Biotechnology*, 27(9), 847–850.
932 <https://doi.org/10.1038/nbt.1561>

933 Quinlan, A. R., & Hall, I. M. (2010). BEDTools: A flexible suite of utilities for comparing
934 genomic features. *Bioinformatics*, 26(6), 841–842.
935 <https://doi.org/10.1093/bioinformatics/btq033>

936 R Development Core Team. (2019). *R: A language and environment for statistical
937 computing*. R Foundation for Statistical Computing, Vienna, Austria. URL <http://www.R-project.org/>. <https://doi.org/10.1007/978-3-540-74686-7>

939 Raudvere, U., Kolberg, L., Kuzmin, I., Arak, T., Adler, P., Peterson, H., & Vilo, J. (2019).
940 g:Profiler: a web server for functional enrichment analysis and conversions of gene lists
941 (2019 update). *Nucleic Acids Research*, 47(1), 191–198.
942 <https://doi.org/10.1093/nar/gkz369>

943 Rausch, T., Zichner, T., Schlattl, A., Stütz, A. M., Benes, V., & Korbel, J. O. (2012). DELLY:
944 Structural variant discovery by integrated paired-end and split-read analysis.
945 *Bioinformatics*, 28(18), 333–339. <https://doi.org/10.1093/bioinformatics/bts378>

946 Reid, B. N., Moran, R. L., Kopack, C. J., & Fitzpatrick, S. W. (2021). Rapture-ready darters:
947 Choice of reference genome and genotyping method (whole-genome or sequence
948 capture) influence population genomic inference in *Etheostoma*. *Molecular Ecology*
949 *Resources*, 21(2), 404–420. <https://doi.org/10.1111/1755-0998.13275>

950 Reid, K., Bell, M. A., & Veeramah, K. R. (2021). *Threespine Stickleback: A Model System
951 For Evolutionary Genomics*. 1–27.

952 Reimegård, J., Kundu, S., Pendle, A., Irish, V. F., Shaw, P., Nakayama, N., Sundström, J.
953 F., & Emanuelsson, O. (2017). Genome-wide identification of physically clustered
954 genes suggests chromatin-level co-regulation in male reproductive development in

955 Arabidopsis thaliana. *Nucleic Acids Research*, 45(6), 3253–3265.
956 <https://doi.org/10.1093/nar/gkx087>

957 Rhie, A., McCarthy, S. A., Fedrigo, O., Damas, J., Formenti, G., Koren, S., Uliano-Silva, M.,
958 Chow, W., Fungtammasan, A., Kim, J., Lee, C., Ko, B. J., Chaisson, M., Gedman, G.
959 L., Cantin, L. J., Thibaud-Nissen, F., Haggerty, L., Bista, I., Smith, M., ... Jarvis, E. D.
960 (2021). Towards complete and error-free genome assemblies of all vertebrate species.
961 In *Nature* (Vol. 592, Issue April, pp. 737–746).
962 <https://doi.org/10.1101/2020.05.22.110833>

963 Roach, M. J., Schmidt, S., & Borneman, A. R. (2018). Purge Haplotigs: Synteny Reduction
964 for Third-gen Diploid Genome Assemblies. *BMC Bioinformatics*, 19(460), 1–10.
965 <https://doi.org/10.1101/286252>

966 Roesti, M., Kueng, B., Moser, D., & Berner, D. (2015). The genomics of ecological vicariance
967 in threespine stickleback fish. *Nature Communications*, 6(1), 1–14.
968 <https://doi.org/10.1038/ncomms9767>

969 Roesti, M., Moser, D., & Berner, D. (2013). Recombination in the threespine stickleback
970 genome - Patterns and consequences. *Molecular Ecology*, 22(11), 3014–3027.
971 <https://doi.org/10.1111/mec.12322>

972 Ronco, F., Matschiner, M., Böhne, A., Boila, A., Büscher, H. H., Indermaur, A., el Taher, A.,
973 Malinsky, M., Ricci, V., Kahmen, A., Jentoft, S., & Salzburger, W. (2020). Drivers and
974 dynamics of a massive adaptive radiation in African cichlid fish. *Nature*, 1–6.
975 <https://doi.org/10.1038/s41586-020-2930-4>

976 Sagonas, K., Meyer, B. S., Kaufmann, J., Lenz, T. L., Häslер, R., & Eizaguirre, C. (2020).
977 Experimental parasite infection causes genome-wide changes in DNA methylation.
978 *Molecular Biology and Evolution*, 37(8), 2287–2299.
979 <https://doi.org/10.1093/molbev/msaa084>

980 Samonte-Padilla, I. E., Eizaguirre, C., Scharsack, J. P., Lenz, T. L., & Milinski, M. (2011).
981 Induction of diploid gynogenesis in an evolutionary model organism, the three-spined
982 stickleback (*Gasterosteus aculeatus*). *BMC Developmental Biology*, 11, 1–11.
983 <https://doi.org/10.1186/1471-213X-11-55>

984 Shapiro, M. D., Marks, M. E., Peichel, C. L., Blackman, B. K., Nereng, K. S., Jónsson, B.,
985 Schluter, D., & Kingsley, D. M. (2004). Genetic and developmental basis of evolutionary
986 pelvic reduction in threespine sticklebacks. *Nature*, 428, 717–723.
987 <https://doi.org/10.1038/nature04500>

988 Sherry, S. T., Ward, M.-H., Kholodov, M., Baker, J., Phan, L., Smigelski, E. M., & Sirotkin, K.
989 (2001). dbSNP: the NCBI database of genetic variation. *Nucleic Acids Research*, 29(1),
990 308–311. <http://www.ncbi.nlm.nih.gov/SNP>.

991 Simão, F. A., Waterhouse, R. M., Ioannidis, P., Kriventseva, E. v., & Zdobnov, E. M. (2015).
992 BUSCO: Assessing genome assembly and annotation completeness with single-copy
993 orthologs. *Bioinformatics*, 31(19), 3210–3212.
994 <https://doi.org/10.1093/bioinformatics/btv351>

995 Smit, A., Hubley, R., & Green, P. (2015). RepeatMasker Open-4.0. In *RepeatMasker Open-4.0*.

997 Spitz, F., Gonzalez, F., Peichel, C., Vogt, T. F., Duboule, D., & Zákány, J. (2001). Large
998 scale transgenic and cluster deletion analysis of the HoxD complex separate an

999 ancestral regulatory module from evolutionary innovations. *Genes and Development*,
1000 15(17), 2209–2214. <https://doi.org/10.1101/gad.205701>

1001 Springer, N. M., Anderson, S. N., Andorf, C. M., Ahern, K. R., Bai, F., Barad, O., Barbazuk,
1002 W. B., Bass, H. W., Baruch, K., Ben-Zvi, G., Buckler, E. S., Bukowski, R., Campbell, M.
1003 S., Cannon, E. K. S., Chomet, P., Kelly Dawe, R., Davenport, R., Dooner, H. K., Du, L.
1004 H., ... Brutnell, T. P. (2018). The maize w22 genome provides a foundation for
1005 functional genomics and transposon biology. *Nature Genetics*, 50(9).
1006 <https://doi.org/10.1038/s41588-018-0158-0>

1007 Stamatakis, A. (2014). RAxML version 8: A tool for phylogenetic analysis and post-analysis
1008 of large phylogenies. *Bioinformatics*, 30(9), 1312–1313.
1009 <https://doi.org/10.1093/bioinformatics/btu033>

1010 Stanke, M., Diekhans, M., Baertsch, R., & Haussler, D. (2008). Using native and syntenically
1011 mapped cDNA alignments to improve de novo gene finding. *Bioinformatics*, 24(5), 637–
1012 644. <https://doi.org/10.1093/bioinformatics/btn013>

1013 Stapley, J., Reger, J., Feulner, P. G. D., Smadja, C., Galindo, J., Ekblom, R., Bennison, C.,
1014 Ball, A. D., Beckerman, A. P., & Slate, J. (2010). Adaptation genomics: The next
1015 generation. *Trends in Ecology and Evolution*, 25(12), 705–712.
1016 <https://doi.org/10.1016/j.tree.2010.09.002>

1017 Stern, D. ben, & Lee, C. E. (2020). Evolutionary origins of genomic adaptations in an
1018 invasive copepod. *Nature Ecology and Evolution*, 4(8), 1084–1094.
1019 <https://doi.org/10.1038/s41559-020-1201-y>

1020 Treangen, T. J., & Salzberg, S. L. (2012). Repetitive DNA and next-generation sequencing:
1021 Computational challenges and solutions. *Nature Reviews Genetics*, 13(1), 36–46.
1022 <https://doi.org/10.1038/nrg3117>

1023 Valiente-Mullor, C., Beamud, B., Ansari, I., Frances-Cuesta, C., Garcia-Gonzalez, N., Mejia,
1024 L., Ruiz-Hueso, P., & Gonzalez-Candelas, F. (2021). One is not enough: On the effects
1025 of reference genome for the mapping and subsequent analyses of short-reads. *PLoS
1026 Computational Biology*, 17(1), 1–29. <https://doi.org/10.1371/JOURNAL.PCBI.1008678>

1027 Vezzi, F., Narzisi, G., & Mishra, B. (2012). Reevaluating Assembly Evaluations with Feature
1028 Response Curves: GAGE and Assemblathons. *PLoS ONE*, 7(12), 1–11.
1029 <https://doi.org/10.1371/journal.pone.0052210>

1030 Walker, B. J., Abeel, T., Shea, T., Priest, M., Abouelliel, A., Sakthikumar, S., Cuomo, C. A.,
1031 Zeng, Q., Wortman, J., Young, S. K., & Earl, A. M. (2014). Pilon: An integrated tool for
1032 comprehensive microbial variant detection and genome assembly improvement. *PLoS
1033 ONE*, 9(11). <https://doi.org/10.1371/journal.pone.0112963>

1034 Wang, Z., Pascual-anaya, J., Zadissa, A., Li, W., Niimura, Y., Huang, Z., Li, C., White, S.,
1035 Xiong, Z., Fang, D., Wang, B., Ming, Y., Chen, Y., Zheng, Y., Kuraku, S., Pignatelli, M.,
1036 Herrero, J., Beal, K., Nozawa, M., ... Wang, J. (2013). The draft genomes of soft-shell
1037 turtle and green sea turtle yield insights into the development and evolution of the turtle-
1038 specific body plan. *Nature Genetics*, 45(6), 701–706. <https://doi.org/10.1038/ng.2615>

1039 Yu, G., Smith, D. K., Zhu, H., Guan, Y., & Lam, T. T. Y. (2017). Ggtree: an R Package for
1040 Visualization and Annotation of Phylogenetic Trees With Their Covariates and Other
1041 Associated Data. *Methods in Ecology and Evolution*, 8(1), 28–36.
1042 <https://doi.org/10.1111/2041-210X.12628>

1043

1044

1045 **Tables and Figures**

1046

1047 **Table 1. Assembly Statistics**

	Contig Assembly	Anchored Assembly
Number of contigs	1906	877 ^a
Total size of contigs	458064828	458376166
Longest contig	5194525	33170598
N50	746270	18858959
		1051
Assembly validation		
Complete BUSCOs	4363	1052 (95.2%)
Complete single-copy BUSCOs	3913	1053 (85.4%)
Complete duplicated BUSCOs	450	1054 (9.8%)
Fragmented BUSCOs	93	1054 (2.0%)
Missing BUSCOs	128	1055 (2.8%)
Total BUSCO groups searched	4584	1056

^a21 LGs, chrM, and 855 unplaced contigs.

1057

1058

1059

Table 2. Distribution of outlier windows and differentially methylated sites (DMS), overlapping genes, and their functional enrichment.

Population Origin	Reference Origin	Metric	Outlier Windows	Outlier Genes	1-1 Ortholog Outlier Genes	Shared Outlier Orthologs	Percentage Overlapping Outliers	Significant GO Terms	Overlapping Terms
North America	North America	Tajima's <i>D</i>	878	1019	335	221	65.97%	3	0
North America	Europe	Tajima's <i>D</i>	874	916	333		66.37%	0	
Europe	North America	Tajima's <i>D</i>	1308	1321	342	214	62.57%	0	0
Europe	Europe	Tajima's <i>D</i>	1309	1449	424		50.47%	3	
North America	North America	F_{ST}	446	541	194	99	51.03%	0	NA
North America	Europe	F_{ST}	440	534	174		56.90%	0	NA
Europe	North America	F_{ST}	672	703	240	101	42.08%	0	0
Europe	Europe	F_{ST}	660	788	243		41.56%	2	
North America	North America	π	888	696	212	29	13.68%	0	NA
North America	Europe	π	880	558	153		18.95%	0	
Europe	North America	π	1332	581	143	36	25.17%	0	NA
Europe	Europe	π	1320	630	199		18.09%	0	
Europe	North America	DMS	2404	712	299	204	68.23%	5	
Europe	Europe	DMS	2550	711	298		68.45%	3	3

Table 3. Distribution of structural variants and structurally variable genes and their functional enrichment.

Population Origin	Reference Origin	SV Type	Number of SVs	Number of SVGs	1-1 Ortholog SVGs	Shared Outlier Orthologs	Percentage Overlapping	Significant GO Terms	Overlapping Terms
North America	North America	Deletion	3915	3034	920	330	35.87%	3	3
North America	Europe	Deletion	5720	2613	877		37.63%	13	
Europe	North America	Deletion	4049	2968	893	296	33.15%	1	0
Europe	Europe	Deletion	5027	2113	716		41.34%	16	
North America	North America	Duplication	2684	3908	1195	500	41.84%	0	NA
North America	Europe	Duplication	3402	3180	1125		44.44%	0	
Europe	North America	Duplication	4300	4070	1256	524	41.72%	2	0
Europe	Europe	Duplication	4425	3072	1074		48.79%	0	
North America	North America	Inversion	794	4128	1358	626	46.10%	20	0
North America	Europe	Inversion	757	3382	1234		50.73%	10	
Europe	North America	Inversion	828	4031	1352	522	38.61%	15	0
Europe	Europe	Inversion	685	2991	1081		48.29%	0	

1 **Figure Legends**

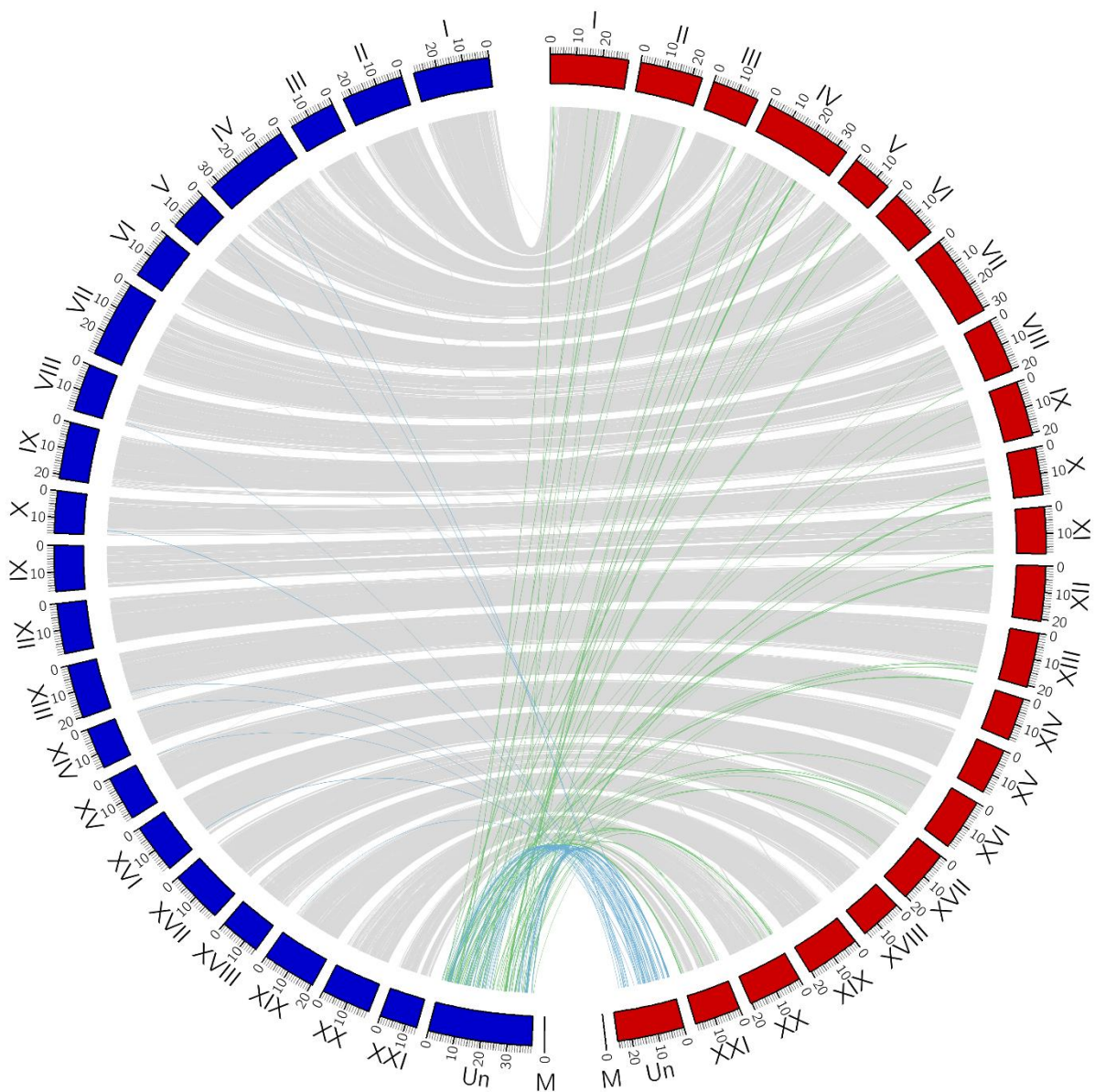
2 **Figure 1. Synteny plot between the two *G. aculeatus* genome assemblies.** Grey lines between the
3 autosomes represent +99% syntenic blocks greater than 1kb between the European gynogen assembly
4 (left, blue blocks) and the North American *G. aculeatus* assembly (right, red blocks). Coloured lines
5 represent synteny between resolved regions and the unmapped scaffold in each assembly. Specifically,
6 blue and green lines represent 1kb +99% syntenic blocks between the unmapped scaffolds and the
7 alternate reference autosome.

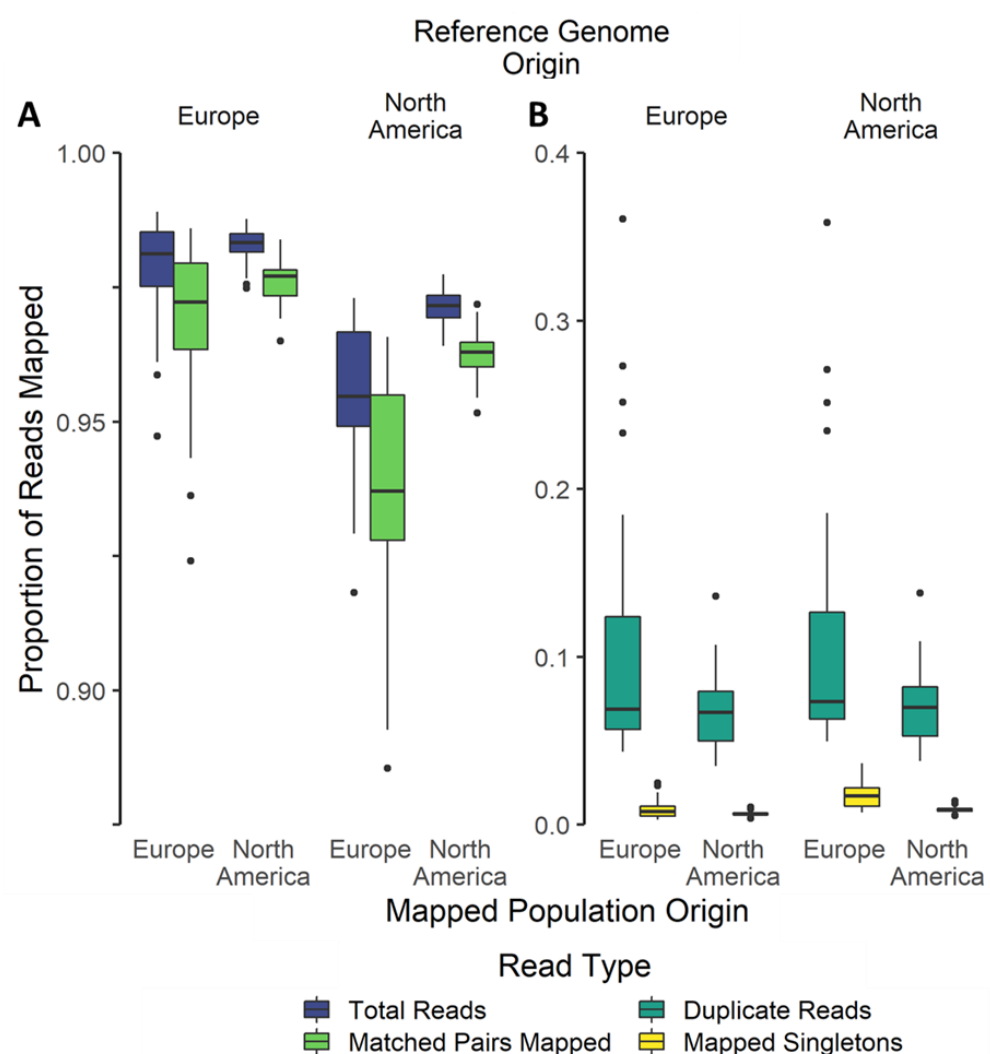
8 **Figure 2. The effect of reference genome origin on mapping efficiency.** Scales differ among panels,
9 but the units are the same (A-B). There was significantly higher mapping efficiency when using the
10 European reference genome regardless of sample origin for total reads (matched and singleton),
11 matched pair reads (A) as well as significantly lower singletons (B). There was no difference in the
12 number of duplicate reads identified. Reference genome origin is labelled at the top of the plot, and
13 mapped population origin at the bottom.

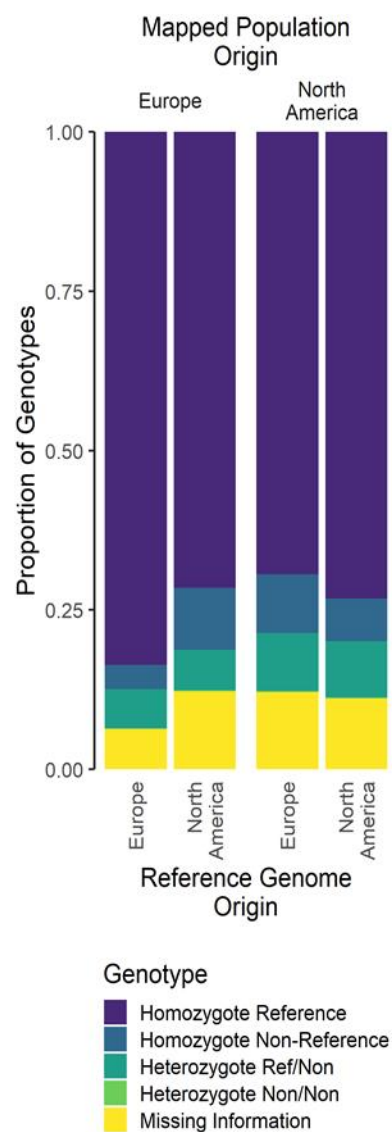
14 **Figure 3. The proportion of SNP classes among all segregating sites.** Segregating sites with no
15 coverage or with a SNP that was removed during filtering are defined as missing information.

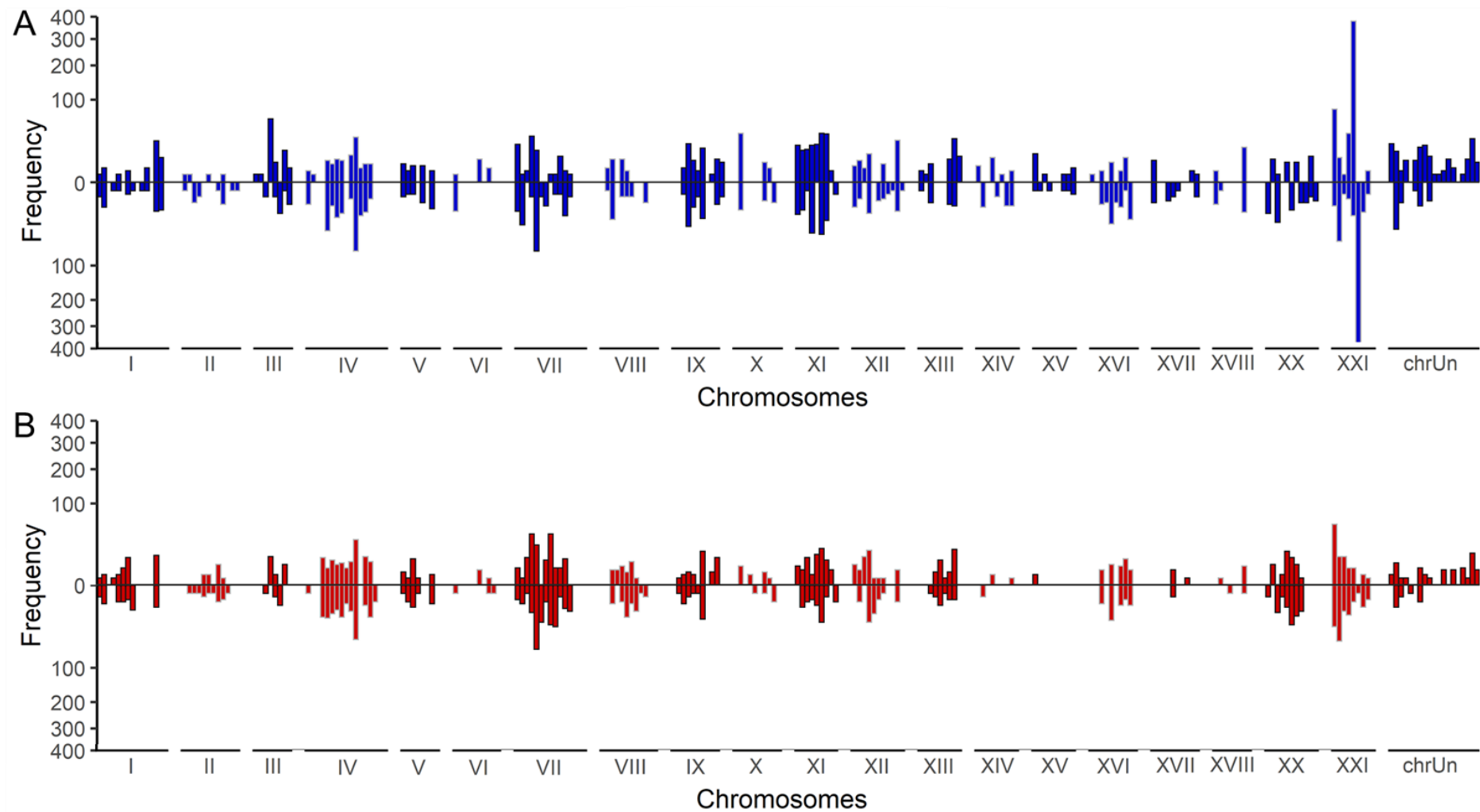
16 **Figure 4. Comparing distributions of π outliers.** Windows are compared across the genome for (top)
17 European and (bottom) North American populations mapped to the (A) European or (B) North American
18 reference genome. Axes are square root transformed.

19









24

25